

*Taxonomic and functional diversity in
Calogaya (lichenised Ascomycota) in dry
continental Asia*

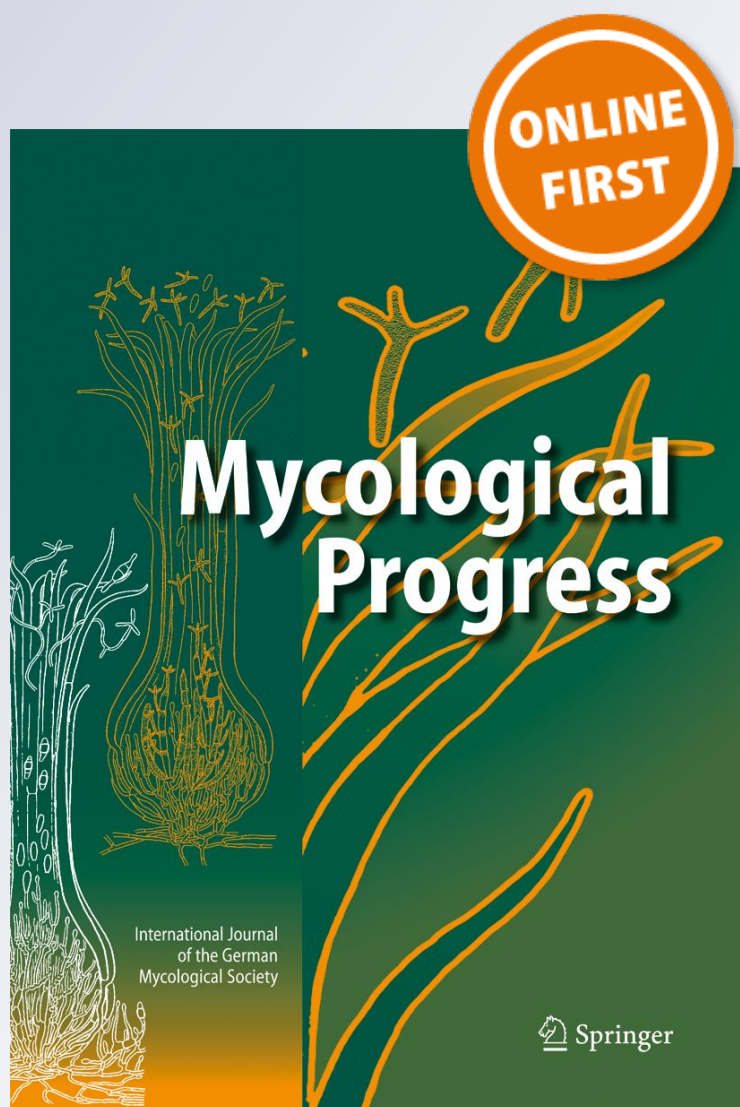
**Jan Vondrák, Hurnisa Shahidin, Mahroo
Haji Moniri, Gökhan Halıcı & Jiří
Košnar**

Mycological Progress

ISSN 1617-416X

Mycol Progress

DOI 10.1007/s11557-018-1402-9



 Springer

Your article is protected by copyright and all rights are held exclusively by German Mycological Society and Springer-Verlag GmbH Germany, part of Springer Nature. This e-offprint is for personal use only and shall not be self-archived in electronic repositories. If you wish to self-archive your article, please use the accepted manuscript version for posting on your own website. You may further deposit the accepted manuscript version in any repository, provided it is only made publicly available 12 months after official publication or later and provided acknowledgement is given to the original source of publication and a link is inserted to the published article on Springer's website. The link must be accompanied by the following text: "The final publication is available at link.springer.com".

Taxonomic and functional diversity in *Calogaya* (lichenised Ascomycota) in dry continental Asia

Jan Vondrák^{1,2}  · Hurnisa Shahidin³ · Mahroo Haji Moniri⁴ · Gökhan Halıcı⁵ · Jiří Košnar²

Received: 16 October 2017 / Revised: 5 March 2018 / Accepted: 13 April 2018
© German Mycological Society and Springer-Verlag GmbH Germany, part of Springer Nature 2018

Abstract

The genus *Calogaya* (Teloschistaceae, Xanthorioideae) was established to accommodate mainly epilithic lichens with lobate thalli, previously regarded as the “*Caloplaca saxicola* group.” Data supporting the recognition of this new genus came from European lichens, and although the genus is soundly based, we have found in Asia numerous epiphytic lineages and lineages with reduced, non-lobate thallus in dry continental areas. The taxonomic and functional diversity of *Calogaya* is distinctly higher in steppe and desert areas of Asia than in the less arid regions of Europe. We sampled 238 specimens, mostly from arid regions of north-western China, Iran, southern Siberia and Turkey. Three nuclear DNA loci were analysed separately and jointly by Bayesian inference, maximum likelihood and *BEAST approaches. Delineations of 28 putative species were tested by BP&P multispecies coalescent model with joint analysis of species delimitation and species-tree estimation. Finally, we recognised 22 taxonomic units: 16 are at species rank, 3 are treated as subspecies and 3 are complexes, treated here as a single entity, but in reality probably including more than one species. *Calogaya altynis*, *C. biatorina* subsp. *asiatica*, *C. decipiens* subsp. *esorediata*, *C. haloxylonis*, *C. orientalis*, *C. xanthoriella* and *C. xinjiangis* are newly described. *Caloplaca zoroasteriorum* is combined into *Calogaya*, and *Calogaya persica* is reduced to a subspecies. The taxonomic status of *Calogaya saxicola* is unclear, and the name is employed here “sensu lato” for several non-monophyletic epilithic lineages with short-lobed thalli. *Calogaya biatorina* and *C. ferrugineoides* are the two other heterogeneous taxonomic units probably including more species.

Keywords *Caloplaca saxicola* · Functional traits · Species concept · Intraspecific taxa · Taxonomic units · New taxa

Section Editor: Gerhard Rambold

Electronic supplementary material The online version of this article (<https://doi.org/10.1007/s11557-018-1402-9>) contains supplementary material, which is available to authorized users.

✉ Jan Vondrák
j.vondrak@seznam.cz

- ¹ Institute of Botany, Academy of Sciences of the Czech Republic, Zámek 1, CZ-252 43 Průhonice, Czech Republic
- ² Department of Botany, Faculty of Science, University of South Bohemia, Branišovská 1760, CZ-370 05 České Budějovice, Czech Republic
- ³ Hurnisa Shahidin, College of Life Science and Technology, Xinjiang University, 830046, Urumqi, China
- ⁴ Mahroo Haji Moniri, Department of Biology, Faculty of Sciences, Mashhad Branch, Islamic Azad University, Rahnamaie Str., Mashhad 917 56 87 119, Iran
- ⁵ Gökhan Halıcı, Department of Biology, Faculty of Science, Erciyes University, Kayseri, Turkey

Introduction

Lichen diversity research in dry continental areas of temperate Eurasia has been largely neglected. This is especially true for the large family Teloschistaceae. Since Magnusson (1940, 1944), few authors have studied Teloschistaceae in these areas, though some recent papers have described particular species from dry continental areas (e.g. Frolov et al. 2016; Kondratyuk et al. 2013; Shahidin et al. 2010; Søchting and Figueras 2007; Vondrák et al. 2013b). In our experience, Teloschistaceae often dominate the biotopes in various steppe and desert areas in Eurasia, and its genera *Calogaya*, *Pyrenodesmia* and *Xanthocarpia* are common and diverse there, apparently more diverse than previously assumed. We found high diversity of *Calogaya* in arid regions of China, Iran, Turkey and southern Siberia. As well as taxonomic diversity, we also observed high functional diversity, i.e. diversity in characters determining niches that the lichen may

occupy and how it interacts with other organisms. Our new data change considerably the overall character of the genus.

Calogaya, as proposed by Arup et al. (2013), was defined as a monophyletic group in a phylogenetic analysis of three loci including mainly epilithic species with conspicuous lobate thalli. Their results supported the view that *Calogaya* mostly contains species formerly grouped in *Gasparrinia* or the *Caloplaca saxicola* group (Gaya 2009; Gaya et al. 2011). These species share the lobate thallus as the most distinct character. Although most DNA sequence data provided by Arup et al. (2013) and Gaya et al. (2011) were from European and North American lobate lichens, sequencing of numerous non-lobate Teloschistaceae populations and data from GenBank revealed that *Calogaya* also includes three non-lobate species: (1) *Calogaya bryochryson* (= *C. alaskensis*), a sorediate arctic-alpine crust with a circumpolar distribution (recently combined into *Calogaya* by Vondrák et al. 2016); (2) *C. schistidii* forming a yellow, usually non-lobate crust over bryophytes; (3) *C. ferrugineoides*, a crust with a reduced thallus surrounding apothecia. The latter was described from Central Asia by Magnusson (1944) and sequence data (ITS barcode) were provided by Vondrák et al. (2012). *Calogaya* sensu Arup et al. (2013) contains only two species producing vegetative diaspores (*Calogaya bryochryson* and *C. decipiens*).

Arup et al. (2013) reported five epilithic species, five epiphytic species (including muscicolous *C. schistidii*) and one species that can be both epiphytic and epilithic (*C. bryochryson*). Whilst all epilithic species occur also in Europe (not in a dry continental climate), three of the epiphytic species are restricted to dry continental regions in Eurasia (*Calogaya ferrugineoides*, *C. persica* and *C. polycarpoides*; Steiner and Poelt 1982; Vondrák et al. 2012).

This paper deals with the taxonomy of *Calogaya*, mainly with taxa occurring in dry continental regions of Eurasia. We evaluate further the variation in substrate preferences (epiphytic vs. epilithic, the former is rather frequent in *Calogaya*), presence of vegetative diaspores and thallus complexity. Finally, we discuss the generic, species and infraspecific concepts in *Calogaya*.

Materials and methods

Sampling

DNA sequence data were obtained from 238 specimens including 84 from Turkey, 74 from NW China (Xin-Jiang), 30 from Iran and 25 from Russia (mainly southern Siberia). The remaining specimens came mainly from Europe. Specimen data to new sequences are listed in Supplementary Table 1.

Molecular protocols

DNA was extracted with a CTAB-based protocol (Aras and Cansaran 2006). Three nuclear DNA loci were amplified: beta-tubulin and MS204 genes and rDNA ITS1-5.8S-ITS2 (ITS barcode). PCRs were performed in a reaction mixture containing 2.5 mM MgCl₂, 0.2 mM of each dNTP, 0.3 μM of each primer, 0.5 U Taq polymerase (Top-Bio, Praha, Czech Republic) in the manufacturer's reaction buffer and sterile water to make a final volume of 10 μL. Primers and cycling conditions are summarised in Table 1. Successful amplifications were sent for Sanger sequencing (GATC Biotech, Konstanz, Germany). The amplification primers were used as the sequencing primers.

Alignments

Sequences were edited in BioEdit 7.2.5 (Hall 1999) and aligned by MAFFT version 7 (Katoh and Standley 2013; available online at <http://mafft.cbrc.jp/alignment/server/>) with L-INS-i method (Katoh et al. 2005). Gaps were coded as a binary data in SeqState v.1.4.1 using simple coding (Simmons and Ochoterena 2000). For the concatenated dataset analysis, we used specimens with sequence data from at least two of the three loci (153 specimens). Single-gene analyses included 201 sequences of ITS, 167 sequences of beta-tubulin and 116 sequences of MS204. We also placed our ITS sequences into the context of the GenBank dataset. For this purpose, we assembled a large alignment of 256 sequences including 205 of our sequences and 51 available GenBank sequences (*Calogaya* and related genera; see Fig. 1). Lengths of alignments and numbers of variable positions are summarised in Table 2. *Rusavskia elegans* was used as outgroup in all alignments.

Phylogenetic analyses

Phylogenetic reconstructions were carried out using maximum likelihood (ML) and Bayesian inference. Models of nucleotide substitutions (Table 2) were selected using AIC criterion implemented in jModelTest v.0.1.1 (Posada 2008). Maximum likelihood analysis of the concatenated alignment (Supplementary Fig. 1) was carried out in RAxML-III (Stamatakis et al. 2005). Bootstrap support was calculated from 1000 replicates. Bayesian analysis was performed using MrBayes 3.1.2 (Huelsenbeck and Ronquist 2001; Ronquist and Huelsenbeck 2003). It was employed for all datasets: the "large" ITS alignment containing available GenBank sequences (Fig. 1), the single-gene alignments (Fig. 2, Supplementary Figs 2-4) and concatenated alignment (Fig. 3). Analyses were performed using two independent runs with four MCMC chains. Trees were sampled after every 500th generation. The analyses were stopped when

Table 1 Sequenced loci; employed primers and PCR parameters

Locus	Primers	PCR settings
MS204	MS204-T-F1 (forward): GGTGACTTCTCTCGCAACCA; MS204-T-R1 (reverse): CCAGCTTGCCCATCCAG (both designed in this study)	95 °C-10 min; 45×: 95 °C-30 s, 52 °C-30 s, 72 °C-60 s; 72 °C-10 min
nrITS	ITS1F (forward): CTTGGTCATTAGAGGAAGTAA; ITS4 (reverse): TCCTCCGCTTATTGATATGC (both published by Gardes and Bruns 1993)	94 °C-3 min; 7×: 94 °C-30 s, 62 °C-30 s (temperature was decreased by 1 °C in each subsequent cycle), 72 °C-60 s; 38×: 94 °C-30 s, 56 °C-30 s, 72 °C-60 s; 72 °C-10 min
Beta-tubulin	Bt3LM (forward): GAACGTCTACTTCAACGAG; Bt10LM (reverse): TCGGAAGCAGCCATCATGTTCTT (both published by Myllys et al. 2001)	94 °C-10 min; 40×: 94 °C-30 s, 52 °C-30 s, 72 °C-60 s; 72 °C-10 min

the average standard deviation of the split frequencies between the simultaneous runs dropped below 0.01. The first 25% of trees were discarded as the burn-in phase, and the remaining trees were used for construction of a 50% majority consensus tree.

Phenotype descriptions

Methods for phenotype description follow Vondrák et al. (2013a). All observations were done on hand-cut sections in water, without any chemical treatments. Measurements are accurate to 0.5 µm for cells, and 1 or 10 µm for larger structures. All measurements of cells include their walls, except for tissues with glutinized cell walls. In each sample, ten or more measurements were done for each measurable character (rarely fewer, when measurable objects were scarce). Following Ekman (1996), results of measurements are given as (min–) X1–X2–X3 (–max), where X1 is the lowest specimen arithmetic mean observed, X2 is arithmetic mean of all observations and X3 is the highest specimen arithmetic mean observed. Total number of measurements (N), number of investigated samples (n) and standard deviation from all measurements (SD) are given for each measured character in square parenthesis [N ; n ; SD]. Morphological terminology follows Smith et al. (2009) and Vondrák et al. (2013a).

Species delimitation

Bayesian phylogeny based on the concatenated dataset of ITS, beta-tubulin and MS204 sequences served as phylogenetic hypothesis for testing species delimitations. Twenty-seven groups resolved in the concatenated tree plus one putative subspecies unresolved within *Calogaya persica* were tested for species delimitation (see below).

*BEAST as implemented in BEAST v.2.4.5 (Drummond and Rambaut 2007) was run on the three-loci concatenated dataset of 153 specimens (the same as employed for Bayesian inference). We used the Strict Clock model, the

Yule model, constant population function and default values for the remaining priors. Two independent MCMC analyses were performed for a total of 10,000,000 generations, sampling every 5000th steps. Convergence of the two runs and the adequacy of sampling were assessed with Tracer v.1.6 (Rambaut et al. 2014). After removing the first 20% of the samples as burn-in, the runs were combined to generate posterior probabilities of nodes from the sampled trees using TreeAnnotator v.2.4.5 (Rambaut and Drummond 2009).

The putative taxa were evaluated using Bayesian MCMC analysis for multi-locus data under the multispecies coalescent model (Rannala and Yang 2003; Yang and Rannala 2010). The joint analysis of species delimitation and species-tree estimation (Yang and Rannala 2014) was conducted using the program BP&P v.3.1 (Yang 2015). This method accommodates uncertainty in the species phylogeny as well as lineage sorting due to ancestral polymorphism, though we are aware of the fact that species delimitation methods based on multi-species coalescent (including BP&P) tend to delimit structure than species (Sukumaran and Knowles 2017); these methods tend to support infraspecific lineages as species.

The species tree inferred by *BEAST was used as a starting tree. The rjMCMC algorithm 1 ($\alpha = 2$, $m = 1$) was used to change the species delimitation model, and the NNI/SPR move was used to change the species-tree topology. Species model prior was set to equal probabilities for rooted trees. A gamma prior $G(1, 20)$, with mean $1/20 = 0.05$ (one difference per 20 bp), was used on the population size parameters. The age of the root in the species tree was assigned the gamma prior $G(2, 2000)$ which means 0.1% of sequence divergence, whilst the other divergence time parameters were assigned the Dirichlet prior (Yang and Rannala 2010: Eq. 2). Mutation rate among loci was specified using random-rates model ($\alpha = 20$). The first 8000 MCMC iterations were set as burn-in. A total of 200,000 post burn-in iterations were carried out, and MCMC samples were taken in each iteration. The analysis was run three times to confirm consistency between runs. The groups with posterior probability consistently exceeding a threshold of 0.95 were declared as distinct taxa.

Fig. 1 Large ITS DNA Bayesian tree based on analysis of our new sequences together with available GenBank sequences. Branches with high posterior probabilities (PP > 0.95) are drawn in thick lines. Clades recognised at the species level are collapsed into triangles of identical vertical dimension. Grey triangles indicate previously known taxa, previously unknown taxa are in black. Length of triangles (horizontal dimension) reflects number of haplotypes within clades. Numbers of samples per clade are in brackets following names of taxa. Outgroup includes closest genera of the subfamily *Xanthorioideae*. (See the “Methods” section and Table 2 for more details)

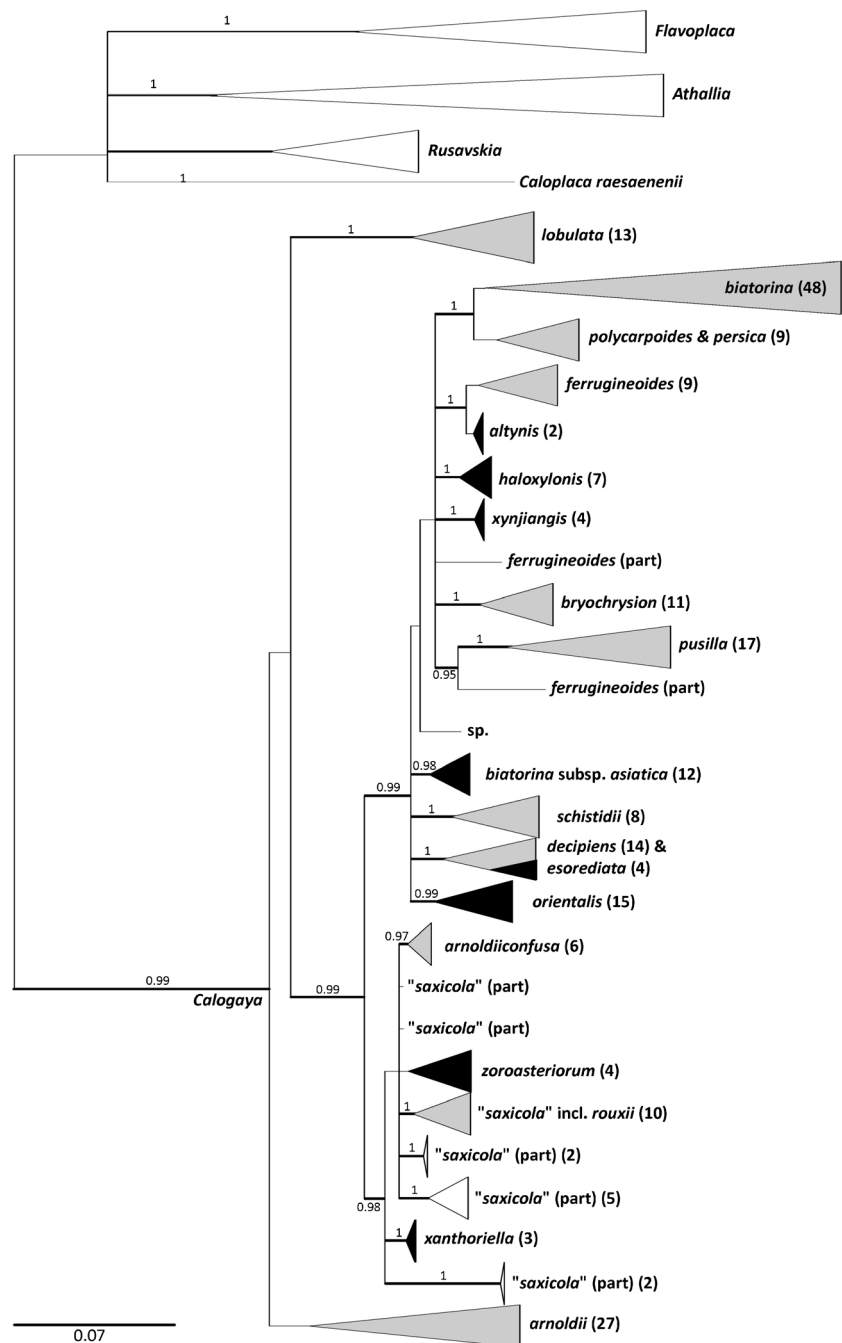


Table 2 Basic information on alignments

Alignment	Number of sequences	Length of alignment/ indel codes	Variable positions (all /in group only)	Parsimony informative positions (all/in group only)	Nucleotide substitution model
nrITS “large”	256	589/144	513/458	369/307	GTR + I + G
nrITS	201	559/78	364/348	225/206	GTR + G
beta-tubulin	167	533/2	172/166	131/130	GTR + G
MS204	116	696/25	312/300	243/216	HKY + G
concatenated (nrITS/beta- tubuline/MS204)	153	1797/88	814/716	535/493	GTR + G/GTR + G/SYM + I + G

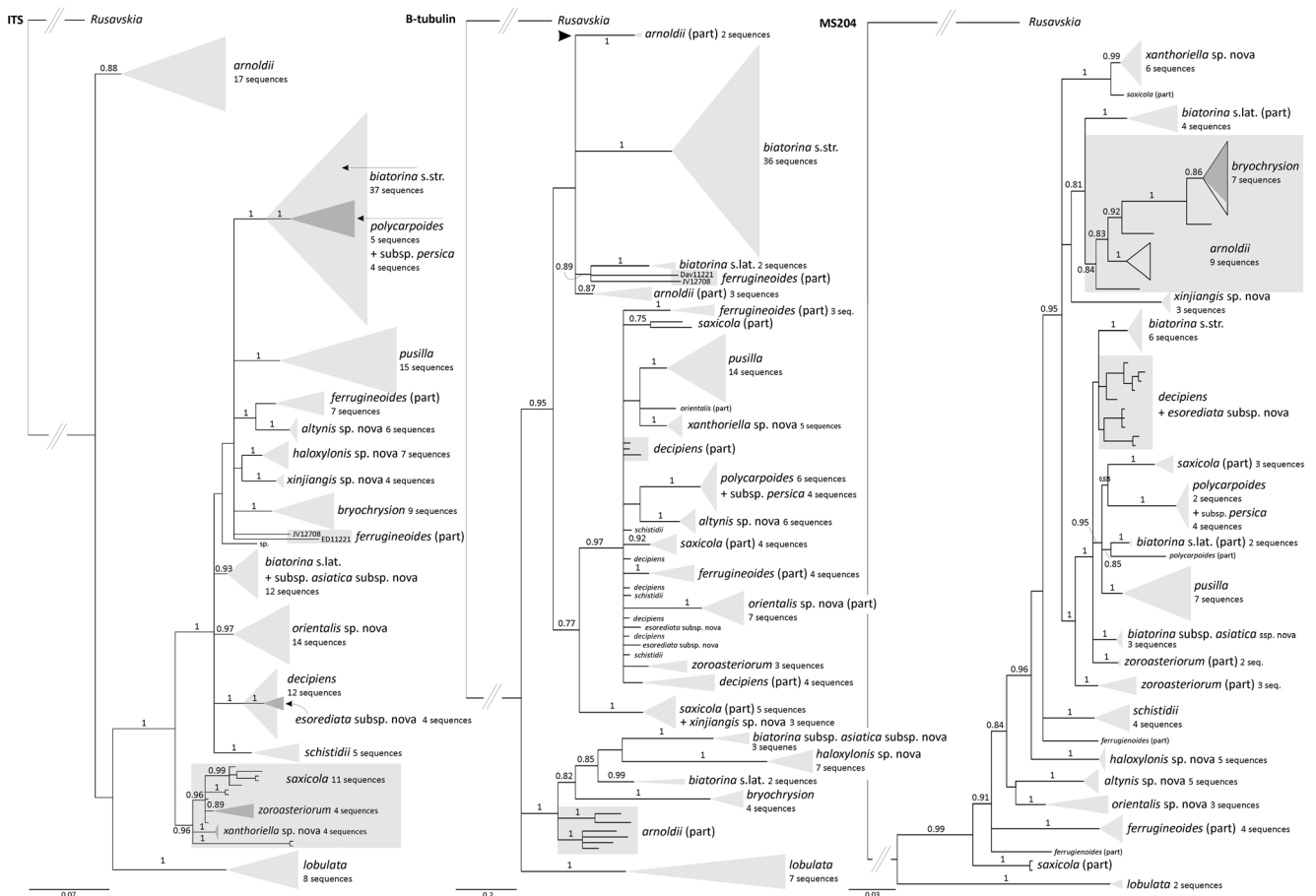


Fig. 2 Single-gene trees generated by Bayesian inference (ITS, on the left; beta-tubulin, in the middle; MS204, on the right). Posterior probabilities (PP > 0.75) drawn at branches. Clades recognised as taxa are displayed as cartoons (triangles). Length of cartoons (horizontal

dimension) reflects number of haplotypes within clades. Height of cartoons reflects sampling size. (More details in the “Methods” section, Table 2 and Supplementary Figs. 2–4)

Defining taxonomic units

On the basis of our data analyses, most specimens are classified as species or subspecies, but some are unresolved and kept in species complexes. An example of a species complex is phenotypically defined *Caloplaca saxicola* that is split into several lineages in phylogenetic trees; each of these lineages may represent a separate species (see the “Results” section). For describing taxonomy and variability in functional traits, we decided to employ a term “taxonomic unit” (OTU in the sense of Sokal and Sneath 1963) including subspecies, species and unresolved species complexes and putting them on the same level. If we only consider resolved species, we lose information.

Results

Large ITS phylogeny

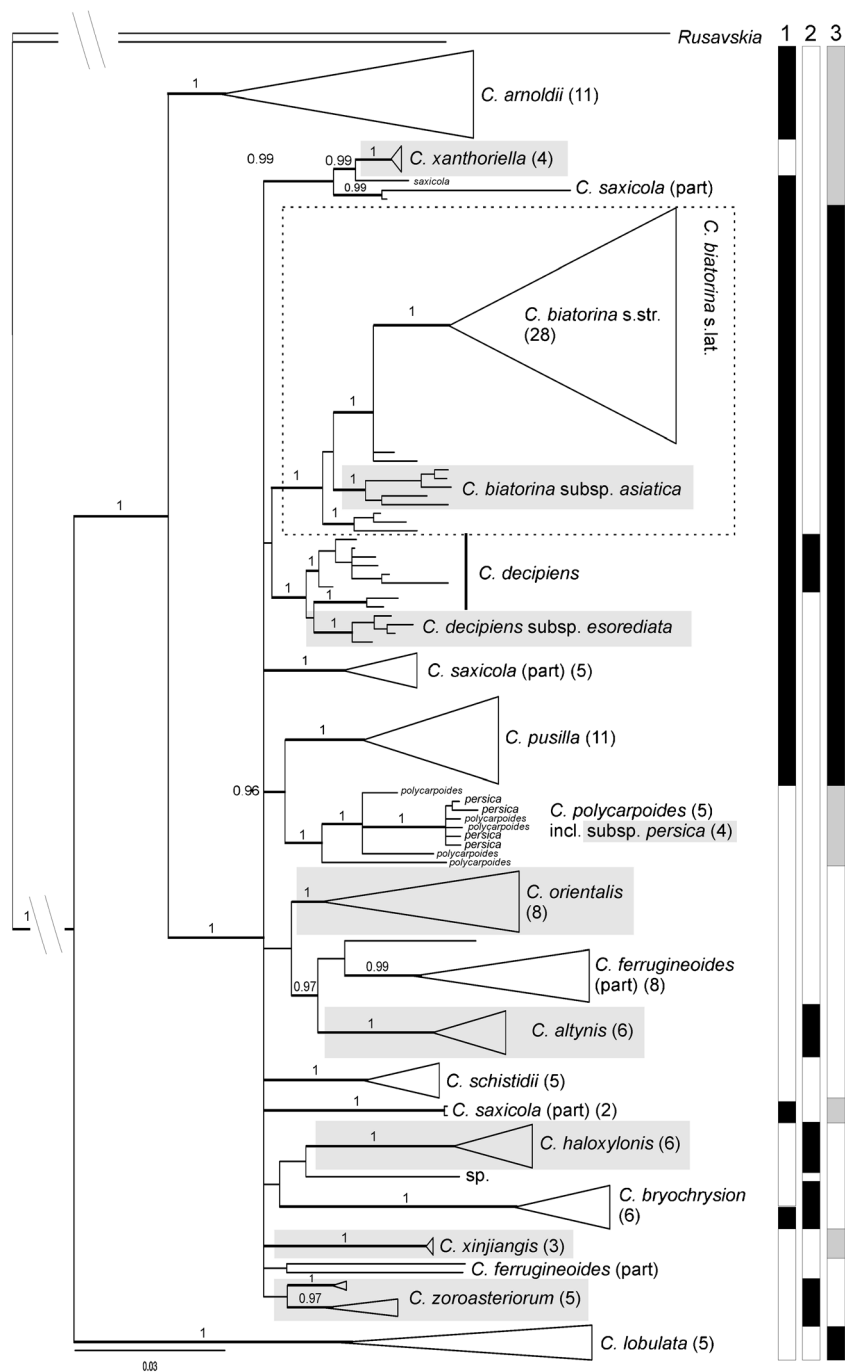
Bayesian analysis of the large ITS sequence dataset including NCBI data showed the relationships of our sequences to

Calogaya sequences available in GenBank. The reconstructed tree (Fig. 1) contains 21 main monophyletic groups within *Calogaya* and a few lineages represented by only one terminal. Eleven of them were previously recognised as species by Gaya et al. (2011) and/or Arup et al. (2013); grey groups in Fig. 1. Another seven are newly recognised here (black groups in Fig. 1). Further lineages are lumped under the name *Calogaya saxicola* which is employed here for a heterogeneous group of lichens with small thalli and short lobes. The previously recognised European species *C. arnoldii confusa* and *C. rouxii*, were not found in arid continental territories.

Single-locus and concatenated phylogenies

All generated phylogenetic trees had an unresolved backbone. If the unsupported nodes (posterior probabilities (PPs) < 0.95) are collapsed in Figs 2 and 3, most putative species-level groups stand in polytomy. *Calogaya arnoldii* and *C. lobulata* are however resolved in most analyses as sister groups to the rest of the taxa. Although the single-loci trees are not fully congruent (Fig. 2; Supplementary Figs. 2–4), the

Fig. 3 Concatenated Bayesian tree based on analysis of alignment including all three loci (ITS, beta-tubulin, MS204). Branches with posterior probabilities (PP > 0.95) are drawn by thick lines. Clades recognised on species level are mostly displayed as cartoons (triangles). Length of cartoons (horizontal dimension) reflects number of haplotypes within clades. Height of cartoons reflects sampling size. Numbers of samples per clade are in brackets following names of taxa. Clades and names shaded in grey represent new taxa or taxa newly combined into *Calogaya*. Columns on the right represent selected phenotype expressions: (1) substrate linkage: black—inorganic, white—organic; (2) vegetative diaspores: black—present, white—absent; (3) thallus complexity: black—always lobate thalli, white—thalli always without lobes, grey—intermediate, some specimens with lobes or lobes poorly developed



differences are mostly in poorly supported topologies which entitles us to use the concatenated tree (Fig. 3) as a reasonable phylogenetic hypothesis for testing species delimitation. Twenty-seven groups resolved in the concatenated tree plus *Calogaya polycarpoides* unresolved within *Calogaya persica* were tested for their delimitation.

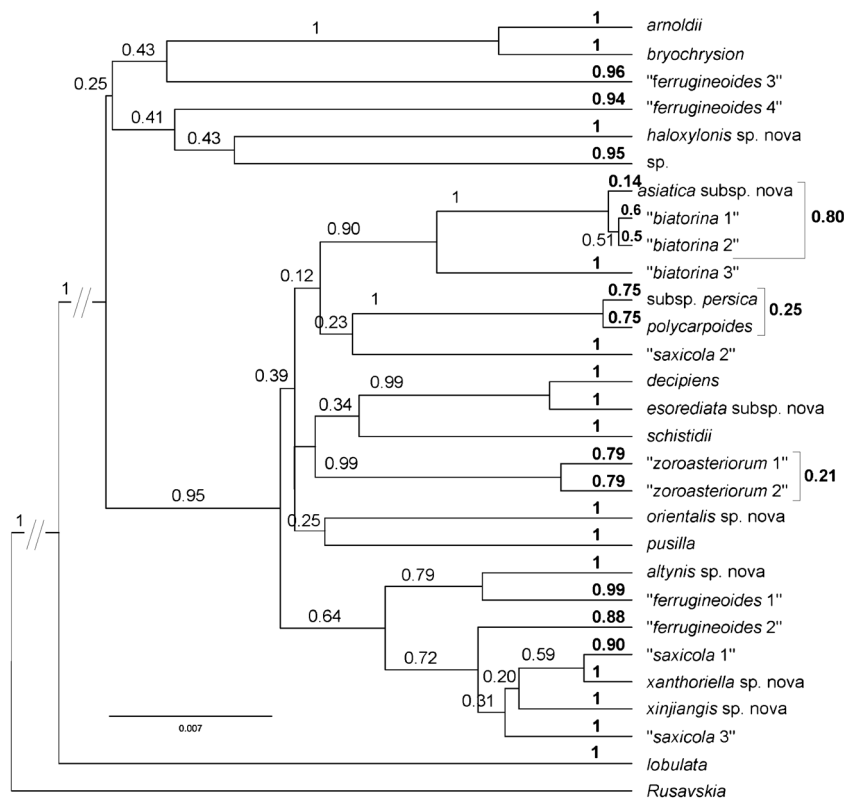
The topology of the trees based on three-loci dataset was largely congruent between the Bayesian inference (Fig. 3) and the species-tree estimation using *BEAST (Fig. 4). Both trees showed poorly supported or unresolved backbone. The

differences were found in poorly supported nodes, and the only exception was the sister relationship between *C. arnoldii* and *C. bryochryson* revealed in *BEAST.

BP&P species delimitation

Out of the 28 putative species based on phylogenetic analysis of the concatenated dataset, 16 were resolved as distinct species with posterior probabilities (PPs) exceeding 0.95 (numbers in italics in Fig. 4). The resolved distinct species

Fig. 4 Species tree inferred from three loci dataset (ITS, beta-tubulin, MS204). Numbers in normal font at each node are *BEAST posterior probabilities. Numbers in bold in front of terminals or behind clamps are BP&P posterior probabilities referring to delimitation of putative species



included six lineages which have not been recognised in previous treatments and which are described here as new taxa (*C. altynis*, *C. decipiens* subsp. *esorediata*, *C. haloxylonis*, *C. orientalis*, *C. xanthoriella*, *C. xinjiangis*). Among the traditionally recognised species, the rank of species was confirmed for six taxa (*C. arnoldii*, *C. bryochryson*, *C. decipiens*, *C. lobulata*, *C. pusilla* and *C. schistidii*). The rank of species was further confirmed for two putative species with the morphology of *C. ferrugineoides* and for two with the morphology of *C. saxicola*. For another nine putative species, the rank of species was found as the most probable solution, although the support was weak as PP values did not exceed 0.95, which could be due to lack of data (only one or few specimens sampled per lineage). Those putative species included lineages with the morphology of *C. ferrugineoides* (2 lineages) or *C. saxicola* (1 lineage) and one lineage similar to *C. polycarpoides* with a single terminal (*Calogaya* sp.; XJUNALH 144878). Among the four putative species morphologically more or less matching *C. biatorina*, the lineage with distinct *C. biatorina* morphology (*C. biatorina* sensu stricto) was resolved as a distinct species. The remaining three putative species, including a lineage with distinct morphology described here as subsp. *asiatica*, were not sufficiently resolved in the analysis, although merging them into a single species received higher support (PP = 0.80) than a split into individual species. Also, no significant solution was found for the two lineages within *C. zoroasteriorum* or for distinguishing *C. persica* from *C. polycarpoides*. The two lineages present

within morphologically defined *C. zoroasteriorum* received higher support when considered as a separate species (PP = 0.79 for both) than when merged as a single species (PP = 0.21). Similarly, in *C. polycarpoides*, the analysis showed higher support for treating subsp. *polycarpoides* and subsp. *persica* as separate species (PP = 0.75 for both) than when merged as a single species (PP = 0.25).

Taxonomic units

Parts of *Calogaya* remain taxonomically unresolved, and we decided to employ taxonomic units instead of species for demonstration of general results. We recognised taxonomic units on three levels (Table 3): species (16), subspecies (3) and species complexes (3). The rank of species was accepted for the lineages with distinct phenotype that are supported in the concatenated tree (Fig. 3). All these lineages are resolved as distinct species in BP&P analysis (PP > 0.95; Fig. 4). *Calogaya polycarpoides* and *C. zoroasteriorum*, even though not supported by BP&P, are considered species because both form units with homogeneous phenotype and both tend to form clades in most analyses (Figs 1, 2, 3 and 4). The rank of subspecies was employed for three groups of specimens with distinct phenotype that do not form distinct lineage supported in the concatenated tree. Species complexes are defined by phenotype similarity. Resolving the taxonomy within these complexes will require future studies based on more extensive sampling.

Table 3 Characters of recognised taxonomic units in *Calogaya*. Names of newly described taxa and new combinations are in italics. Phylogenetic support: *M* monophyly, *N* in grey non-monophyly, (*M*) monophyly with low support, ? missing data, *grey shading* unsupported; Functional traits: *Y* presence of character, *N* absence of character

Taxonomy		Phylogenetic support					Functional traits			
Rank	Taxonomic units	nrITS	B-tubulin	MS204	Concatenation	BP&P posterior probabilities	Organic substrate	Thallus reduction	Vegetative diaspores	
Species	<i>altynis</i>	M	M	M	M	1	Y	Y	Y	
	<i>arnoldii</i>	M	N	N	M	1	N	N/Y	N	
	<i>arnoldiiconfusa</i>	M	?	?	?	?	N	N	N	
	<i>biatorina sensu stricto</i>	N	M	M	M	1	N	N	N	
	<i>bryochryson</i>	M	M	M	M	1	N/Y	Y	Y	
	<i>decipiens</i>	M	N	N	M	1	N	N	Y	
	<i>esorediata</i>	M	N	M	M	1	N	N	N	
	<i>haloxylonis</i>	M	M	M	M	1	Y	Y	Y	
	<i>lobulata</i>	M	M	M	M	1	Y	N	N	
	<i>orientalis</i>	M	N	M	M	1	Y	Y	N	
	<i>polycarpoides</i>	M	M	N	M	0.25	Y	N/Y	N	
	<i>pusilla</i>	M	M	M	M	1	N	N	N	
	<i>rouxii</i>	M	?	?	?	?	N	N	N	
	<i>schistidii</i>	M	N	M	M	1	Y	Y	N	
	<i>xanthoriella</i>	M	M	M	M	1	Y	N/Y	N	
	<i>xinjiangis</i>	M	N	M	M	1	Y	N/Y	N	
	<i>zoroasteriorum</i>	(M)	?	N	(M)	0.21	Y	Y	Y	
Subspecies	<i>biatorina subsp. asiatica</i>	N	M	M	M	0.14	N	N	N	
	<i>polycarpoides subsp. persica</i>	N	N	N	N	0.75	Y	N/Y	N	
Species complexes	<i>biatorina sensu lato</i>	N	N	N	M	< 0.01	N	N	N	
	<i>ferrugineoides sensu lato</i>	N	N	N	N	< 0.01	Y	Y	N	
	<i>saxicola</i>	N	N	N	N	< 0.01	N	N/Y	N	

Functional diversity

Functional traits, such as substrate preferences, reproductive mode and thallus reduction, are more diverse in *Calogaya* than suggested from mostly European sampling (Table 4). *Calogaya* has been considered predominantly epilithic, but our data revealed six new epiphytic species from continental parts of Eurasia. All of them have reduced thallus without or at most with traces of lobes (only two non-lobate species known before) and three of them produce vegetative diaspores (two species known before).

We report only two new subspecies from inorganic substrata, but several saxicolous lineages requiring further appraisal were found in the *C. biatorina* and *C. saxicola* species complexes. Most recognised saxicolous species have a lobate thallus, but morphotypes with fully reduced lobes are present within *C. arnoldii* and *C. saxicola* species complexes. We did not reveal any new epilithic lineages with vegetative diaspores.

Distribution of substrate preferences, reproductive modes and thallus reduction were mapped on the concatenated phylogenetic tree (Fig. 3, stripes on the

Table 4 Species richness and functional diversity within *Calogaya* in Europe, dry continental Asia and in Eurasia; plus newly recognised part of diversity. Taxonomic units reflect Table 3

Groups of taxonomic units	Europe	Dry continental Asia	Eurasia	Newly revealed
All	9	20	22	9
Epiphytic	3	11	12	6
Without lobate thallus	2	8	8	5
With vegetative diaspores	2	5	5	3
Epiphytic, without lobate thallus	1	7	7	5
Epilithic, strictly without lobate thallus	1	1	1	0

right). The species-level groups are mostly characterised by the substrate. They grow either on inorganic substrata (14 lineages/10 taxonomic units; including European *C. arnoldii* and *C. rouxii*) or on organic substrata (15 lineages/12 taxonomic units), usually on trees and shrubs but also on wood and over bryophytes and organic soil. Some exceptions exist: members of epilithic lineages are exceptionally found on tree bark or wood (e.g. dust impregnated) in communities with other epilithic lichens. *Calogaya bryochryson* is an exceptional species in the genus growing, like numerous other arctic alpine lichen species, on both organic and inorganic substrata (see Vondrák et al. 2016).

Species in *Calogaya* are also characterised either by the presence (5 taxa) or absence (17) of vegetative diaspores and by the level of thallus reduction. Thallus lobes, always present in e.g. *C. biatorina*, are always absent in e.g. *C. haloxylonis*, and the thallus is always reduced to a thalline apothecial margin in *C. orientalis*. In *C. arnoldii* and in the *C. saxicola* species complex, the thallus may be lobate or not (already revealed by Gaya 2009).

Discussion

Generic concept

In the rather recent past, lichenologists employed some unreasonably large genera (Arcadia 2009), but they have been, or are starting to be, split up in recent decades (e.g. Crespo et al. 2010). The three main genera of *Teloschistaceae*, *Caloplaca* including crustose lichens, *Xanthoria* with foliose lichens and *Teloschistes* with fruticose ones, were reorganised into 39 genera (Arup et al. 2013). The old system had polyphyletic genera, some of which were also inconveniently large (*Caloplaca* had about 1000 species), and the new taxonomy proposed by Arup et al. (2013) is undoubtedly an improvement. It has been criticised because it left “gaps” in the taxonomic space within *Teloschistaceae*. Many species that do not belong in *Caloplaca* s. str. were not combined elsewhere and remain, uncomfortably, in *Caloplaca* s. lat., but these species are gradually being combined into new genera (e.g. Søchting et al. 2014a, b). Another criticism is that some of the new genera do not have any diagnostic morphological synapomorphies, and species were placed in them using only DNA evidence. This is to some extent the case for *Calogaya* and most other genera in *Xanthorioideae*. However, any alternative taxonomy would also have problems of their own, and we consider that distinguishing the genera related to *Calogaya*, e.g. *Athallia* and *Flavoplaca*, still makes a good deal of sense. *Flavoplaca* tends to be strictly saxicolous and contains either sorediate/blastidiate crusts or predominantly species with strongly reduced thallus. *Athallia* tends to have strongly reduced thalli without vegetative diaspores. *Calogaya* tends to

form lobate thalli, at least in epilithic species, whereas lobate thalli are exceptional in *Athallia* and *Flavoplaca*. The three genera also have reasonable sizes including tens of species (Arcadia 2009).

Other ideas about splitting *Teloschistaceae* were put forward in Kondratyuk et al. (2014a, b). Kondratyuk's taxonomy is mostly independent of the one proposed by Arup et al. (2013) and uses distinctly smaller genera, often monotypic (Kondratyuk et al. 2015a, b). (For example, Kondratyuk et al. 2015a described a new genus *Lazarenkoella* to accommodate a single species *L. zoroasteriorum* that is undoubtedly within *Calogaya*; see our data). We are not persuaded that this degree of splitting is a constructive approach to the taxonomy of *Teloschistaceae*. (Incidentally, *Lazarenkoella* is based on sequence data that do not belong to *Calogaya zoroasteriorum* but to another *Calogaya*; see the note in our taxonomic treatment). Although *Calogaya* forms a well supported group within *Xanthorioideae* (Figs. 1, 2 and 3), the relationships among its species are mostly unresolved, and we can see no justification for splitting *Calogaya* into smaller units, such as *Lazarenkoella*.

Species concept

Gaya et al. (2011) attempted to incorporate the results of ITS phylogeny of the *Caloplaca saxicola* group (now a part of *Calogaya*) into the traditional species concept, raising distinct morphotypes and ecotypes to species level. She recognised eight species, most of them monophyletic, but *Caloplaca saxicola* was paraphyletic with nested *Caloplaca rouxii* in all analyses. As in our study, relationships between most species remained unresolved. The species concept proposed by Gaya et al. (2011) was based on clusters of similar sequences (usually monophyletic groups) with a phenotypic sense, i.e., differing from other clusters by phenotype. This concept was maintained by Arup et al. (2013) for the whole of *Calogaya* including some ten species. It is also maintained by us so far as possible, though we note that it may fail in some of the cases. As the amount of sequence data available increases (by addition of specimens from new substrata or regions), new lineages of *Calogaya* will be detected in phylogenetic reconstructions and it becomes less easy to decide which lineages should be regarded as species. For example, many lineages have the “*Calogaya saxicola*” appearance; some others appear indistinguishable from *C. ferrugineoides*. We have formally named as species most lineages with significant BP & P support that can be circumscribed by phenotype (mostly by some combination of thallus appearance, presence/absence of vegetative diaspores, substrate preferences and geographical range). Several clades with insufficient information (including only one or few terminals) or clades indistinguishable from *C. ferrugineoides* or *C. saxicola* sensu Gaya (2009) are left for future appraisal (taxonomic units in rank “species

complex” in Table 3). In Teloschistaceae, we have experienced similar difficulties for *Pyrenodesmia*, *Rufoplaca*, *Rusavskia*, *Xanthocarpia* and other taxa (data not published) when a sequence dataset has been extended.

Infraspecific taxa

Here, we employ the rank “subspecies” for all phenotypically distinct taxa that are not clearly separated from another taxon by our three-loci concatenated analysis nor by BP&P (Table 3). Lücking (2008) proposed a well thought out but rather strict system for infraspecific ranks, in which subspecies is to be used only for phenotypically distinct and allopatric populations of the same species, variety for distinct phenotypes with overlapping but different geographic ranges and forma for distinct phenotypes that do not differ in distribution. However, this scheme does not offer any rank for taxa with the same phenotype and distribution but differing in substrate, presumably because Lücking did not consider that purely ecological barriers to gene flow exist, in which case such “taxa” could not be taxonomically distinct. Lücking’s scheme may work well in some groups of lichens, but in our experience, it does not work for all. There is evidence for the existence of purely ecological barriers to gene flow in some cases: specificity of closely related populations to different substrata is a common case in Teloschistaceae (Gaya et al. 2015) including *Calogaya*. Moreover, other kinds of barriers may exist, for example modifications in genome size that are common in fungi (e.g. Veselská et al. 2014) including lichenized fungi (our unpublished data on Teloschistaceae). Another sympatric crossing barrier is provided by different reproduction mode of infraspecific taxa: crossing is strongly restricted if at least one of the infraspecific populations has strongly reduced sexuality (vegetative reproduction predominant).

Our main reason for employing only one infraspecific level is that there is very little knowledge about gene flow between infraspecific taxa of the same species in *Calogaya*, so it would be hard to justify a more complicated scheme at present. We definitely do not wish to ignore infraspecific taxa entirely, because of their possible significance for biodiversity. For instance, Tehler et al. (2013) did not recognise vegetatively reproducing populations in several *Dirina* species at any infraspecific level, which leads to the loss of ecological information when records are made, because vegetatively reproducing populations (at least in *D. fallax* and *D. massiliensis*) have different ecological and geographical ranges: unlike sexual populations, which are only coastal, asexual *Dirina* also occurs far inland.

Functional diversity

The functional diversity approach has recently been employed in lichenology (e.g. Bässler et al. 2015; Johansson et al. 2012,

2013; Nelson et al. 2015). Functional traits are characters that influence the role of a particular organism in an environment. Diversity in functional traits provides different information than taxonomical diversity; it describes variability in the adaptations to and the functions of organisms in an environment. For example, numerous lichen species with a simple cladoniiform growth form are favoured by forest fires, but species with more complex growth form (reindeer lichens) are excluded by fires (Nelson et al. 2015). For our purposes in *Calogaya*, we selected the following three functional traits: (1) presence/absence of vegetative diaspores (which determines dispersal ability and ability of generative reproduction, Vondrák et al. 2016); (2) degree of thallus reduction (which reflects ecology of particular species, e.g. epilithic populations below overhangs have generally more reduced thalli than populations on exposed rocks); (3) substrate preferences (which is a derived character influenced by a complex combination of morphological, physiological and other traits, but it is simple and convenient to use and it directly circumscribes a pool of possible niches). In contrast to previous taxonomical treatments (Arup et al. 2013; Gaya 2009), our results revealed that both functional and taxonomic diversity within *Calogaya* known in Europe are distinctly lower than in dry continental regions of Asia. Whilst epiphytic taxa and taxa with reduced, non-lobate thallus are a minority in Europe (in both cases only 2 species), most epiphytic taxa (11) and all known taxa with reduced thallus (8) are present in dry continental Asia. There is a similar but less distinct difference in species producing vegetative diaspores (Tables 3 and 4). Thallus reduction, i.e. absence of thallus lobes, was more frequently observed in epiphytic populations (in 7 of 12 taxonomic units) than in epilithic (1 of 10). This is consistent with Vondrák et al. (2012): it is not possible to put a large crustose thallus onto a small twig where many epiphytic *Calogaya* prefer to grow.

Taxonomy

New taxa

Data for appraised specimens (herbarium, specimen accession number, geography, altitude, co-ordinates) and NCBI’s accession numbers to their sequences are in Supplementary Table 1.

Calogaya altynis H. Shahidin, **species nova**

Mycobank: MB820485.

Fig. 5a, b

Type: CHINA. Xinjiang: Kunlun Mts (Karakorum), alt. 3830 m, 36.5175 N, 76.6166666E, on twigs of *Krascheninnikovia ceratoides*, 20 June 2008, *Abdulla Abbas 20080634* (**holotype** XJU-NALH)

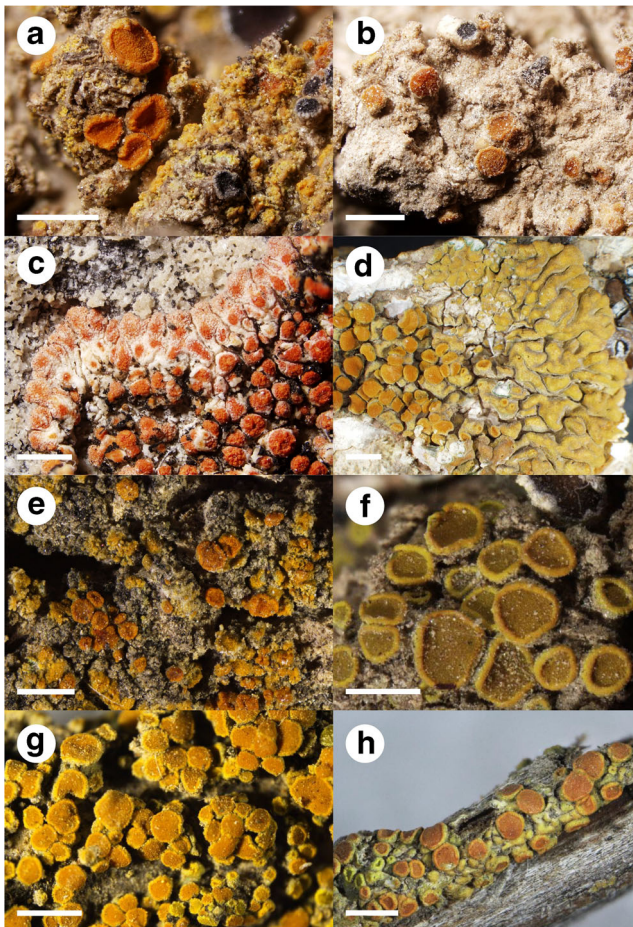


Fig. 5 **a** *Calogaya altynis* (XJU-NALH 20081049–6), morphotype with blastidia. **b** The same specimen, morphotype with inconspicuous thallus. **c** *C. biatorina* subsp. *asiatica* (PRA JV12707). **d** *C. decipiens* subsp. *esorediata* (Mahroo 3164). **e** *C. haloxylonis* (holotype). **f** *C. orientalis* (XJU-NALH 20136740). **g** *C. xanthoriella* (XJU-NALH 20081367). **h** *C. xinjiangis* (XJU-NALH 20136641). Bar, 1 mm

Type sequences: KY748973 (ITS), KY748759 (beta-tubulin), KY748917 (MS204)

Etymology: “altynis” is the genitive singular case of the noun Altyn (mountains in China in the geographical range of *C. altynis*).

Short diagnosis: Thallus of scattered areoles or granules (Fig. 4a), often restricted to a few areoles around apothecia, sometimes hardly visible (Fig. 4b). Bright yellow to orange blastidia formed at the margins of areoles. Apothecia dispersed, zeorine, 0.3–0.9 mm diam. Disk flat to concave, dark orange to orange, thalline exciple light orange, thin, sometimes sorediate. True exciple paler or of the same colour as the disk. Asci with 8 ascospores. Ascospores polarilocular, 10–17 × 5–7 μm, length/width ratio 1.9–3.0; septum 2.0–3.4 μm

Ecology and distribution: Three localities known in alpine desert in Altyn Mts (Altyn-Tagh) and Karakorum Mts, at altitudes 3730–4160 m. Growing on stems and twigs of old shrubs *Krascheninnikovia ceratoides*.

Phylogeny: *Calogaya altynis* forms a well supported clade in the single-locus trees (Fig. 2) and in the concatenated tree (Fig. 3). Its closest relative could be *C. ferrugineoides*; the sister relationship of the two species is supported (pp = 0.97) in the concatenated tree. BP&P supported it as a distinct species (Fig. 4).

Detailed description: Thallus crustose, corticolous, inconspicuous or of scattered areoles, orange to grey, (78–) 164–200–274 (–408) μm in thick [24; 2; 77.5]. Blastidia occur at margin of areoles or as tiny granules directly on substrate, (16–) 31.6–35.9–40.7 (–49) μm diam. [27; 3; 8.3], not always developed (Fig. 4b). True cortex absent; alveolate cortex up to 60 μm thick [20; 2; 11.3], of thick-walled cells, (4.8–) 6.2–9.1–8.4 (–13.8) × (4–) 5–6.4–6.9 (–9.8) μm [23; 2; 2.4&1.7], cell wall (0.4–) 0.62–1–1.16 (–1.9) μm thick [22; 2; 0.36]. Algal layer thin and discontinuous, rarely well developed. Medulla absent.

Apothecia numerous to scarce, sessile, zeorine, (0.25–) 0.5–0.52–0.58 (–1.2) μm diam. [29; 4; 0.19]. Disc flat to slightly convex, dark to light orange. Thalline exciple entire, lower than the true exciple, sometimes eroded into blastidia, lemon yellow to yellowish orange; (49–) 85–86–87 (–116) μm thick in the upper part and (153–) 201–212–221 (–242) μm thick in the lower part [18; 2; 22 and 68]. Cortex of thalline exciple conspicuous near the base, paraplectenchymatous or alveolate, (22–) 31.3–41.9–48.5 (–68) μm thick [25; 3; 12.5], consisting of elongated to almost isodiametric cells, (6.3–) 9.6–10.7–11.5 (–17) × (2.2–) 6–7.1–7.8 (–10.5) μm [21; 3; 2.4 and 2.2], with thick cell walls, (0.5) 1.2–1.3–1.5 (2.2) μm [21; 3; 0.42]. True exciple (parathecium) raising and entire, orange, (28–) 51–54.6–59.7 (–73) μm in wide [18; 3; 13.04], consisting of radiating cells gradually shortened and thicker towards margin, upper 1–2 cell layers firmly covered by anthraquinone pigments, uppermost cells are ± round, (4.3–) 7.2–8.3–9.6 (–12.9) × (3.4–) 5.8–6.3–7.1 (–8.9) μm [19; 3; 2.2 and 1.6], with thick cell walls, (0.5–) 0.76–0.78–0.81 (–1.3) μm [18; 3; 0.22]. Lower part of true exciple indistinct, (7.5) 12.3–13.6–14.6 (23) thick [18; 3; 4.4]. Hymenium colourless, (45–) 55.7–59.4–64.5 (–71.5) μm high [24; 3; 8.3]; Hypothecium (14.3–) 23.7–33.1–38.2 (–55.4) μm high [26; 3; 12], with oil droplets, consisting of ± round, oblong or irregular cells, c. 5–8 × 3–4 μm. Paraphyses usually simple but sometimes branched or forked or anastomosed near base, tip cells usually slightly swollen, rarely almost roundish, (4–) 5.3–6.2–6.4 (–9) μm wide [29; 3; 1.3], basal cells (1.7–) 2–2.1–2.2 (–2.6) μm wide [23; 3; 0.24]. Asci 8 spored, (25–) 45.0–46.3–49.4 (–64) × (10–) 13.6–15–15.2 (–20) μm [34; 3; 6.7&2.6], ascus length/width ratio (2.08–) 3.04–3.16–3.64 (–4.3) [34; 3; 0.55]; Ascospores (8.0–) 13.0–13.6–14.0 (–19.7) × (4.0–) 5.3–5.6–5.7 (–7.2) μm [55; 3; 2.3 and 0.8], ascospore wall (0.4–) 0.63–0.67–0.76 (–1.4) μm [39; 3; 0.17], ascospore length/width ratio (1.6–) 2.42–2.46–2.51 (–3.2) [55; 3; 0.34]. Ascospore septum (1.7–) 2.6–

2.7–2.9 (–4.0) μm [55; 3; 0.5], septum width/ascospore length ratio (0.1–) 0.19–0.21–0.22 (–0.31) [55; 3; 0.05].

Pycnidia rare, reddish orange, of *Xanthoria* type. Conidia ellipsoid, (2.8–) 3.1–3.5–3.6 (–4.0) \times (1.5–) 1.72–1.84–1.9 (–2.3) μm [28; 2; 0.33 and 0.18].

Calogaya biatorina* subsp. *asiatica M. Haji Moniri, Halıcı & Vondrák, **subspecies nova**

Mycobank: MB820486

Fig. 5c

Type: TURKEY. Kahraman Maraş: Nurhak, alt. 2200 m, 38.034300 N, 37.417312E, on limestone in alpine zone, 31 Aug 2014, *J. Vondrák 12670* (**holotype** PRA).

Type sequences: KY749012 (ITS), KY748805 (beta-tubulin), KY748918 (MS204)

Etymology: Epithet refers to Asia; the whole known geographical range of the taxon lies within that continent.

Short diagnosis: Thallus \pm orbicular, orange to red, with lobate margin and areolate central part. Lobes are typically slender, widened at tips, occasionally branched, not imbricate, about 0.4–1.6 mm long and 0.2–0.4 mm wide. Areoles (in central part of thallus) are round, convex and with ribbed surface. White pruina is macroscopically visible towards thalline margin but indistinct in thallus center; often forming a rim between areoles and lobes. Apothecia in thallus centre but also on lobes. Young apothecia urceolate, with deep crevices in thalline exciple, but crevices diminish with age of apothecia. Thalline margin always darker orange than discs. Discs \pm white pruinose. Asci with 8 ascospores. Ascospores polarilocular, ellipsoid, 10–12 μm long on average; length/width ratio 1.9–2.4; spore length/septum width ratio 3.3–4.1. Diagnostic characters against most similar taxa *C. biatorina* subsp. *biatorina* and *C. pusilla* are summarised in Table 5.

Ecology and Distribution: Known only from limestone rocks in dry and continental regions of southern Siberia, NW China and Turkey, often in alpine zone, at altitudes 1310–4830 m.

Phylogeny: Although it forms a supported clade distinct from *C. biatorina* in the single-locus ITS phylogeny (Figs. 1 and 2, left), it is a part of the *C. biatorina* s.lat. clade in the concatenated tree (Fig. 3). BP&P found no significant solution for its status, although merging it into a single species with the other two clades of *C. biatorina* sensu lato received higher support than its treatment as a separate species (Fig. 4).

Detailed description: Thallus crustose, saxicolous, placodioid, with marginal lobes and densely areolate in centre, (0.5–) 1.04–1.16–1.25 (–2) cm diam. [21; 3; 0.42]. Lobes slender, not overlapping, tightly appressed to substrate, (0.1–) 0.45–0.90–1.57 (–1.9) mm long [36; 4; 0.65] and (0.2–) 0.40–0.47–0.50 (–1) mm wide [43; 4; 0.15]. Areoles round, convex, (0.1–) 0.30–0.36–0.42 (–0.9) mm diam. [36; 4; 0.18]. Thickness of thallus (0.11–) 0.27–0.38–0.53 (–0.75) mm [43; 4; 0.18]. Thallus surface rough to ribbed, dark orange or

red, usually white pruinose, but pruina often absent from tops of lobes/areoles. Prothallus not seen. Vegetative diaspores absent. Cortex uneven (10–) 22.8–26.8–30.0 (–65) μm thick [45; 4; 15.4], paraplectenchymatous, of cells (3–) 5.0–6.0–6.5 (–12) $\mu\text{m} \times$ (2–) 3.35–3.80–4.0 (–8) μm [82; 4; 1.8 & 1.14] and containing extracellular crystals 3–8 $\mu\text{m} \times$ 1–4 μm . Epinecral layer usually present, (10–) 23.0–34.3–50.1 (–87) mm thick [38; 4; 63], formed of deformed cortex cell remnants. Algal layer (25–) 53–72–85 (–125) μm thick [45; 4; 24.85]; algal cells globose, (4–) 7.20–9.10–10.10 (–15) μm diam. [66; 4; 2.73]. Medulla well developed, (75–) 154–230–300 (–410) μm thick [41; 4; 93.95]; medullary tissue cellular, formed of loose thin-walled paraplectenchymatus tissue, consisting of cells variable in shape and size and of minute extracellular crystals, c. 1–5 μm diam.

Apothecia usually abundant, (0.10–) 0.26–0.40–0.51 (–0.7) mm diam. [73; 4; 0.15], zeorine to biatorine, at first urceolate becoming sessile to adnate, (0.1–) 0.20–0.32–0.45 (–0.8) mm high [41; 4; 0.17]. Disc orange, flat to convex, even, \pm pruinose. Thickness of medulla under mature discs (35–) 69–98–134 (–175) μm [42; 4; 39.19]. Thalline exciple orange, darker than the disc, prominent, with dense deep cracks (in young apothecia), reduced, with less and thinner cracks (in mature apothecia), (10–) 21–25–30 (–40) μm thick in the middle part [36; 4; 7.98] (in mature apothecia). Cortex of thalline exciple restricted to the lower part, paraplectenchymatous, of thin-walled cells, (3–) 2.8–4.7–5.4 (–8) $\mu\text{m} \times$ (2–) 3.3–4.0–4.6 (–6) μm [50; 4; 1.1 and 1.1]. True exciple (10–) 15.1–16.3–17.2 (–27) μm wide [42; 4; 4.55], colourless, formed of thin-walled paraplectenchymatous tissue in the uppermost part, of cells (2.0–) 3.1–4.5–5.7 (–8.0) μm long \times (1.0–) 2.2–3.0–3.7 (–5.0) μm [47; 4; 1.5 and 1.04]; lower part of palisade prosoplectenchyma of thin-walled cells, (3.0–) 4.2–6.2–7.0 (–10.0) $\mu\text{m} \times$ (1.5–) 2.5–2.6–2.9 (–4.0) μm [57; 4; 1.8 and 0.65]. Hymenium (32–) 52.0–65.0–73.7 (–87) μm thick [39; 4; 14.87]; colourless, glutinized, with extracellular oil drops; uppermost part of hymenium yellow-brown by anthraquinones. Hypothecium (23–) 35–46–66 (–75) μm thick [36; 4; 16] in central part, more or less flat, colourless, formed of thin-walled cells of various shapes and sizes, (3.0–) 3.8–5.1–5.6 (–8.0) $\mu\text{m} \times$ (1.0–) 3.3–3.7–3.8 (–6.0) μm [80; 4; 1.2 and 3.7]; sometimes with glutinized cell walls. Asci of the *Teloschistes* type, clavate to cylindrical, 8-spored, (33–) 48–52–57 (–70) $\mu\text{m} \times$ (11–) 14.3–15.0–15.3 (–23) μm [60; 4; 6.2&2.4]. Ascospores polarilocular, (7.0–) 10.4–11.2–12.1 (–15.0) \times (3.0–) 4.5–5.6–6.4 (–8.0) μm [96; 4; 1.8 and 1.0]; length/width ratio (1.14–) 1.93–2.04–2.37 (–3.50) [96; 4; 0.41]. Ascospore septa (2.0–) 2.8–2.9–3.2 (–5.0) μm wide [96; 4; 0.76]; ratio of septum width/ascospore length (0.14–) 0.25–0.26–0.31 (–0.45) [95; 4; 0.06]; ascospore wall up to 1 μm thick; ascospores usually ellipsoid, but some sandglass, rhomboid and citriform ascospores observed in all samples. Paraphyses usually branched, containing oil droplets, (1.5–)

Table 5 Characters distinguishing *Calogaya biatorina subsp. asiatica* from the most similar *Calogaya* taxa. Character states in italics are considered diagnostic against *C. biatorina subsp. asiatica*

Character	<i>C. biatorina subsp. asiatica</i>	<i>C. biatorina subsp. biatorina</i>	<i>C. pusilla</i>
Thallus colour	Dark orange to red	Orange to reddish-orange	<i>Salmon, ochraceous-yellow or yellow</i>
Thallus size (mm)	10–15	2–20	2–18
Thickness of thallus (µm)	(100) 270–530 (750)	100–250 (300)	100–365
Length/width of lobes (mm); lobe position	0.4–1/0.4–0.5; not imbricate	<i>0.4–3/0.3–1.5, contiguous or imbricate</i>	<i>0.3–1.5/0.2–1.2; contiguous or imbricate</i>
Shape of inner areoles	Round	<i>Angular; polygonal</i>	<i>Irregular; polygonal</i>
Pruina	Macroscopically visible towards thallus margin, but indistinct in thallus centre; often forming a rim between areoles and lobes	Most of Asian specimens not pruinose	Sometimes pruinose and covering whole upper surface in central parts of thallus
Thickness of algal layer (µm)	55–85	40–80	40–125
Apothecium diam. (mm)	0.25–0.5	0.3–0.8	0.2–1.2
Thalline margin	Darker than disk	<i>Paler than disk</i>	<i>Same colour or paler than disk</i>
Ascospore size (µm)	(7)10.4–11.2–12.1(15) × (3)4.5–5.6–6.4(8)	(9)11–12.4–14(16.5) × (5)6.5–7.3–8(9.5)	(9)10.5–11.9–13.5(15.8) × (4.5)5.5–6.3–7(8.7)
Ascospore septum (µm)	(2)2.8–2.9–3.2(5)	(1.5)2–2.7–3.5(4.5)	(2.5)3–3.9–4.5(6)
Length/septum ratio	(2.34–) 3.32–3.93–4.06 (7.0)	(2.7)3.4–4.7–6.2(9.8)	(2.1)2.6–3.1–3.7(4.6)

2.3–2.5–2.7 (–5.0) µm wide in the lower part [69; 4; 0.7]; widened to (3.0–) 3.8–4.6–5.2 (–7.0) µm in the upper part [73; 4; 1.0]; the number of widened cells below the paraphyses tips 0–3; the tips always covered by external anthraquinone pigments. Extracellular crystals ±present in all apothecial parts, c. 1–5 µm diam., with no reaction with sulphuric acid. Pycnidia not seen.

Calogaya decipiens subsp. esorediata* M. Haji Moniri & Vondrák, *subspecies nova

Mycobank: MB820487

Fig. 5d

Type: IRAN. East Azerbaijan Province: Lake Urmia, rocks near road c. 2 km N of Saraydeh, alt. 1280 m, 37.882956 N, 45.573871E, on siliceous rock, 7 May 2007, *J. Vondrák 5822* (**holotype** PRA)

Type sequences: KY749050 (ITS), KY748812 (beta-tubulin), KY748925 (MS204)

Etymology: Epithet refers to the absence of soralia (which are present in *C. decipiens subsp. decipiens*).

Short diagnosis: Forming thick placodioid crust, up to 3 cm diam.; marginal lobes often folded and imbricate; thallus surface matt yellow-ochre, sometimes white pruinose. Orange zeorine apothecia abundant in central part of thallus. Thalline apothecial margin always of the same colour as thallus. Disc distinctly orange, not pruinose. Asci with 8 ascospores. Ascospores polarilocular, ellipsoid, 9.5–10.5 µm long on average; ratio of septum width/ascospore length 0.25–0.35. Similar to *C. decipiens*, but without vegetative propagules.

Ecology and Distribution: Known from siliceous and calcareous rocks in NW and NE Iran, at altitudes 980–1650 m.

Phylogeny: The subspecies *esorediata* forms a strongly supported clade inside the clade of *C. decipiens* in the concatenated tree (Fig. 3). It forms its own clade within *C. decipiens* also in ITS and MS204, but it is unresolved in beta-tubulin (Fig. 2). BP&P supported it as a distinct species (Fig. 4).

Detailed description: Thallus crustose, epilithic, placodioid, rosette forming, imbricate, matt yellow-ochre, densely areolate at the centre. Lobe sides and folds white pruinose, with crystals (3.0–) 3.0–3.2–3.3 (–4.0) cm diam. [5; 2; 0.45]. Prothallus indistinct or absent. Areoles, convex, round, polygonal or irregular (0.2–) 0.58–0.64–0.68 (–1.2) mm [30; 2; 0.29]. Marginal lobes convex, folded, irregularly branched, overlapped, usually broadened towards tips and branching into 1–5 secondary lobules, (0.2–) 0.4–0.6–0.7 (–1.0) mm wide at base [27; 2; 0.29], and (0.5–) 0.9–1.5–1.9 (–3.5) mm wide at tips [30; 2; 0.77]; lobe length (2.0–) 3.5–4.0–4.5 (–7.0) mm [32; 2; 1.29]. Thallus in section (0.2–) 1.1–1.2–1.3 (–2.5) mm [39; 2; 0.67]. Vegetative diaspores absent. Cortex uneven, (15–) 36–41–45 (–75) µm thick [15; 2; 18.9], of thick-walled paraplectenchymatous cells, (3.0–) 8.10–8.11–8.12 (–20.0) × (2.0–) 4.0–4.5–5.0 (–9.0) µm [47; 2; 3.5 and 1.33], with cell wall (1.0–) 1.2–1.4–1.5 (–2.0) µm thick [32; 2; 0.35]; mostly covered with brown-orange epinecral layer, (12–) 24–27–29 (–62) µm thick [22; 2; 13.7]. Algal layer ±continuous, (75–) 117–130–143 (–225) µm thick [15; 2; 41.3], but sometimes divided into indistinct

algal stacks; algal cells globose, (7.0–) 11.0–12.0–12.5 (–22.5) μm diam. [29; 2; 4]. Medulla well developed, loose prosoplectenchyma, (0.3–) 1.1–1.3–1.4 (–2.0) mm thick [20; 2; 0.5], medullary tissue consisting of thin-walled hyphae, (1.5–) 3.2–3.6–3.8–5.0) μm thick [27; 2; 1.12]. Extracellular crystals without reaction to sulphuric acid observed in both cortex and medulla.

Apothecia frequent, mostly aggregated in the central part, dark orange, zeorine to biatorine, round to oval, (0.6–) 1.26–1.26–1.26 (–1.8) mm diam. [21; 2; 0.29], sessile, (0.22–) 0.41–0.43–0.44 (–0.6) mm high [21; 2; 0.10]. Medulla under the apothecium distinct, (0.22–) 0.40–0.42–0.44 (–0.65) mm high [17; 2; 0.13]; formed of hyphae (0.1–) 3.0–3.2–3.5 (–5.0) μm thick [30; 2; 0.89]; sparse minute oil drops and crystals present. Disc orange, flat to convex, even, usually with dotted surface ornamentation, sometimes cracked (also in young apothecia). Thalline exciple more visible in young apothecia, slightly or not prominent in mature apothecia, of the same colour as thallus, (12–) 23–35–47 (–68) μm wide in the middle part [16; 2; 18]. Cortex of thalline exciple formed of thin-walled paraplectenchymatous cells, (5.0–) 7.4–7.5–7.6 (–9.0) \times (3.0–) 4.9–5.2–5.3 (–7.0) μm [24; 2; 1.07 and 0.94]. True exciple yellow to slightly yellow-orange, always paler than the disk, colourless in inner parts, (6.0–) 12.2–12.8–13.3 (–18.0) μm wide [20; 2; 3.65]; formed of thin-walled cells, c. 0.2–0.5 μm thick; with paraplectenchymatous cells in the uppermost part, (3.0–) 4.1–5.7–7 (–12) \times (2.0–) 2.8–3.2–3.5 (–5.0) μm wide [20; 2; 2.2 and 0.95], and clear prosoplectenchymatous tissue in the lowermost part, with cells (5.0–) 7.0–8.1–10.3 (–12.0) \times (2.0–) 3.0–3.2–3.8 (–5.0) μm [27; 2; 2.01 and 0.8] with thick walls, (0.5–) 0.6–0.7–0.8 (–1.0) μm wide [20; 2; 0.13]. Hypothecium usually flat, colourless, (45–) 62–65–69 (–80) μm thick [19; 2; 10.6], formed of cells with different shapes, (2.0–) 5.6–6.2–6.6 (–10.0) \times (2.0–) 3.4–3.7–3.8 (–5.0) μm [30; 2; 2.2 and 0.84]. Hymenium colourless, (50–) 57–60–62 (–79) μm high [22; 2; 8.3], with extracellular crystals of calcium salts, c. 1–2 \times 2–3 μm , with positive reaction to sulphuric acid; some minute dispersed extracellular oil drops present. Paraphyses usually simple, seldom branched, often formed of thin-walled cells, glutinized cell walls not observed (1.0–) 2.0–2.05–2.1 (–3.0) μm wide at base [29; 2; 0.48]; apical cells swollen (3.0–) 3.8–4.2–4.4 (–5.0) μm wide [26; 2; 0.74]; the number of widening cells below the paraphyses tips (1–4) [33; 2; 0.9]; the tips always covered by external anthraquinone pigments. Asci clavate, 8-spored, of *Teloschistes* type, (42–) 54–56–58 (–80) μm high [23; 2; 11.6], and (11.0–) 14.1–14.2–14.2 (–18.0) μm wide [22; 2; 1.7]. Ascospores well developed, polarilocular, (4.0–) 4.8–5.0–5.0 (–6.0) \times (8.0–) 9.7–10.0–10.3 (–12.0) μm [27; 2; 0.7] and [34; 2; 1.43]; length/width ratio (1.4–) 1.9–2.0–2.1 (–3.0) [27; 2; 0.38]; septa (2.0–) 2.4–2.5–2.5 (–3.0) μm thick [28; 2; 0.5]; ratio of septum width/ascospore length (0.17–) 0.25–0.26–0.26 (–0.37)

[16; 2; 0.06]; usually ellipsoid, but citriform, sandglass, and rhomboid shapes rarely present.

Pycnidia frequent (less common than apothecia), (150–) 210–240–275 (–300) μm wide in section through the middle part [9; 2; 52.12], surrounded by cortex, distinguishable on surface by their orange tops contrasting with yellow thallus surface. Conidiophores raised from the compact anastomosed tissue, packed together, various in shape, formed of isodiametric, long or cone-shaped cells, (3.0–) 4.5–4.9–5.0 (–10.0) μm length [30; 2; 1.66]. Conidia usually ellipsoid (1.0–) 1.3–1.4–1.5 (–2.0) \times (2.0–) 2.9–3.0–3.1 (–4.0) μm [30; 2; 0.35 and 0.37].

Calogaya haloxylonis M. Haji Moniri, H. Shahidin & Vondrák, **species nova**

Mycobank: MB820488

Fig. 5e

Type: CHINA. Xinjiang: Dzungaria basin desert, alt. 439 m, 44.412039 N, 87.858391E, on old *Haloxylon persicum* stems, 3 May 2008, A. Abbas, H. H. Shahidin 20080186 (**holotype** XJU-NALH).

Type sequences: KY749022 (ITS), KY748763 (beta-tubulin), KY748896 (MS204).

Etymology: “haloxylonis” means pertaining to *Haloxylon*. Although Greek form of the adjective is “haloxyli”, we prefer to follow Latin grammar.

Short diagnosis: Thallus consisting of minute grey-green to yellow squamules that dissolve into yellow blastidia. Apothecia absent or sparse (rarely aggregated), orange, zeorine. Thalline apothecial margin usually paler than the disk. Asci with 8 ascospores. Ascospores polarilocular, c. 10.5–12.0 \times 5.0–6.0 μm , with septa c. 2.5–3.2 (–5.0) μm , up to 5 μm wide. Pycnidial tops dark orange. Conidia ellipsoid to subglobose c. 1.5–3.0 \times 1.0–1.5 μm .

Ecology and distribution: Known from three localities in NE China (Xinjiang: Dzungaria basin and Tianshan Mts) at altitudes 430–2710 m and once collected in NE Iran at altitude 1550 m. It is a strict epiphyte on twigs and stems of *Haloxylon persicum*, rarely on other woody plants.

Phylogeny: *Calogaya haloxylonis* forms a well-supported clade in the single-locus trees (Fig. 2) and in the concatenated tree (Fig. 3). Its relationships to other *Calogaya* species are unresolved. BP&P supported it as a distinct species (Fig. 4).

Detailed description: Thallus epiphytic, covering up to several centimetres, formed of minute yellow-orange to strongly orange squamules. Squamules usually scattered, not overlapping, (0.1–) 0.3–0.6–0.9 (–1.6) mm wide [59; 4; 0.31], (0.1–) 0.25–0.27–0.3 (–0.4) mm thick [87; 7; 0.07], emerging from \pm hypophloedal yellow-grey hypothallus. Blastidia yellow to grey, formed on margins of squamules or raised directly from hypothallus, (13–) 33.35–37.90–43.20 (–75) μm diam. [51; 4; 18.1]; prothallus not seen. Alveolate cortex conspicuous, uneven, (12–) 26–31–34 (–62) mm [37; 4; 14.3], usually

covered with thin yellow-brown epinecral layer, with dispersed \pm isodiametric crystals of calcium salts, (1.0–) 1.56–2.02–2.20 (–5.0) μm diam. [58; 4; 0.96]. Algal layer uneven, (50–) 107–136–164 (–250) μm thick [34; 4; 59.4]; algal cells (5.0–) 13.4–14.8–16.6 (–30.0) μm diam. [52; 4; 6]. Medulla/algonecral medulla (63–) 124.6–131.9–143.5 (–212) μm thick [36; 4; 42.6]; formed by prosoplectenchymatous tissue, of thin-walled hyphae, (2.00–) 3.14–0.82–3.56 (–5.00) μm diam. [34; 4; 0.82]; with \pm isodiametric dispersed crystals of calcium salts, (1.0–) 2.0–2.54–2.85 (–5.0) μm diam. [52; 4; 1.01]; forming needle-like crystals with sulphuric acid.

Apothecia absent or rather sparse, dispersed to aggregated, zeorine, orange, rounded, (0.3–) 0.51–0.54–0.64 (–1) mm diam. [38; 4; 0.13]. Mature apothecia adnate to sessile, (0.10–) 0.24–0.3–0.34 (–0.75) mm high [25; 2; 0.14]. Medulla below the apothecium distinct, (75–) 130–132–133 (–250) μm high [23; 2; 38.6]; formed of compact isodiametric cells under apothecial edge, becoming loose with long branched hyphae below the apothecial centre; sometimes an uneven layer of isodiametric cells forming the lowest surface. Disc flat to weakly convex, even, not pruinose. Thalline exciple persistent, orange, (20–) 30–80–133 (–195) μm wide in the middle part [32; 6; 30]. Cortex of thalline exciple formed of thick-walled cells variable in shape (rounded to hexagonal) with lumina (3.0–) 4.9–7.6–8.4 (–13.0) $\mu\text{m} \times$ (3.0–) 4.0–5.0–6.0 (–7.0) μm [59; 4; 2.17 & 1.15]; cell walls (0.4–) 0.9–1.3–1.8 (–3.0) μm thick [50; 4; 0.75]; in some parts covered with a light brown epinecral layer c. 5–15 μm thick. True exciple prominent, persistent, colourless, (12–) 19–21–23 (–35) μm wide [21; 2; 6.2]; formed of thin-walled cells in the uppermost part, (3.0–) 4.1–4.6–4.9 (–7.0) $\mu\text{m} \times$ (1.0–) 2.3–2.5–2.8 (–3.0) μm [26; 2; 1.05 and 0.58]; and of elongated thin-walled cells in the lower part, (3.0–) 6.3–6.7–7.0 (–9.0) $\mu\text{m} \times$ (1.0–) 1.9–2.5–2.9 (–4.0) μm [34; 2; 2.17 and 0.86]. Hypothecium flat, colourless, sometimes with weak greyish tinge in the centre or at the base, (20–) 45–56–64 (–100) μm thick [38; 5; 17.4], formed of intricate paraplectenchymatous tissue with thin-walled cells, (3.0–) 5.4–5.7–6.7 (–11.0) $\mu\text{m} \times$ (2.0–) 3.6–3.8–4.1 (–7.0) μm [73; 4; 1.65 and 1.1]. Hymenium colourless, (43–) 52–70–85 (–112) μm high [42; 5; 17.1], with \pm gelatinous matrix and with sparse minute oil drops; extracellular crystals of calcium salts (1.0–) 2.5–3.3–4.1 (–10.0) $\mu\text{m} \times$ (1.0–) 2.1–2.4–2.6 (–5.0) μm [40; 2; 2.2 and 1.25] with no reaction with sulphuric acid. Paraphyses branched, thin-walled but sometimes glutinized, (2.0–) 2.2–2.5–2.6 (–4.0) μm wide [67; 4; 0.56] in lower part, widening gradually to (3.0–) 4.2–5.0–5.6 (–7.0) μm [70; 5; 1.02] in tip cells containing oil drops; 1–2 uppermost cells widened, tips always covered by external anthraquinone pigments. Asci clavate, 8-spored, of *Teloschistes* type, (32–) 42–51–60 (–80) μm tall [66; 5; 8.9], and (8–) 11–14–15 (–20) μm wide [66; 5; 2.8]. Ascospores polarilocular, (7.0–) 10.9–11.3–11.8 (–16.0) \times (3.0–) 5.2–5.5–5.7 (–8.0) μm [119; 5; 1.9 &

1.0], septa (10.0–) 2.5–2.9–3.2 (–5.0) μm [119; 5; 0.72]. Ascospore length/width ratio; (1.14–) 1.94–2.11–2.28 (–4.0) [119; 5; 0.51]; septum width/ ascospore length ratio; (0.08–) 0.23–0.26–0.29 (–0.57) [119; 5; 0.08]. Well-developed ascospores ellipsoid, but rarely citriform or rhomboid ascospores observed.

Conidiomata, pycnidia visible as strong orange spots on thallus surface, (80–) 90–92–93 (–100) μm wide in section through the middle part [13; 3; 8]; surrounded by cortex tissue; pycnidial wall around ostiolum light to dark brownish, otherwise colourless. Conidiophores arranged tightly; conidiogeneous cells variable in shape, \pm isodiametric, thin walled, usually smaller than cortical cells surrounding pycnidium, (2.0–) 3.8–4.1–4.5 (–6.0) μm in size [58; 3; 1.07]. Conidia ellipsoid to subglobose, (1.0–) 1.0–1.28–1.53 (–2.0) \times (1.0–) 1.62–1.28–2.80 (–3.0) μm [35; 3; 0.4 and 0.75].

Calogaya orientalis M. Haji Moniri, H. Shahidin, Halıcı, Vondrák, **species nova**

Mycobank: MB820489

Fig. 5f

Type: CHINA. Xinjiang: westernmost fringe of the Kunlun Shan Mts, Oytagh, alt. 2840 m, 38.898533 N, 75.225833E, on dead wood of *Juniperus centrasitica* in subalpine cold desert, H. Shahidin & A. Abbas 20110301 (**holotype** XJU - NALH).

Type sequences: KY749061 (ITS), KY748770 (beta-tubulin), KY748908 (MS204)

Etymology: Epithet refers to the distribution of *C. orientalis* east of Europe.

Short diagnosis: Unlike other *Calogaya* species, the thallus of *C. orientalis* is largely reduced to a thalline exciple, and this character is most similar to some species of *Athallia*. Muscicolous specimens are morphologically indistinguishable from the alpine *A. saxifragarum*. Corticolous specimens strongly resemble *A. cerinelloides*. Both *Athallia* species have distinctly broader ascospores and wider ascospore septa. Whilst ascospore length/width ratio is about 2–2.3 in *C. orientalis*, it is 1.3–1.7 in *A. cerinelloides* and 1.6–1.8 in *A. cerinelloides*. Ascospore septa are 2–4 μm wide in *C. orientalis* but usually more than 4.5 μm wide in both *Athallia* species (more details for *Athallia* in Vondrák et al. 2012). Some species of *Calogaya* with reduced thallus (e.g. *C. ferrugineoides*) are distinct in having stalked apothecia with high loose medulla underneath; *C. orientalis* usually has sessile apothecia.

Ecology and distribution: All records are from arid steppe/desert habitats in Iran, Turkey and NW China, at altitudes 810–2840 m. Six sampled specimens are muscicolous on calcareous or volcanic outcrops, five are overgrowing plant debris on soil and three are corticolous on shrub twigs or on sunlit bark of solitary trees.

Phylogeny: *Calogaya orientalis* forms a supported clade in all single-locus trees (Figs. 1 and 2) and in the concatenated tree (Fig. 3), with unresolved relationships to other *Calogaya* taxa. BP&P supported it as a distinct species (Fig. 4).

Detailed description: Thallus inconspicuous, thin, film-like, mostly visible only as a white-grey rim around apothecia. Cortex developed only in thalline exciple; distinct algal layer and medulla only present below apothecia. Algal cells globose (10.0–) 14.1 (–17.5) μm diam [60; 1; 3.3]. Prothallus indistinct from thallus. Vegetative diaspores absent.

Apothecia orange, zeorine to biatorine, dispersed to aggregated in groups, rounded to slightly ellipsoid, (0.45–) 0.74–0.75–0.96 (–1.30) mm diam. [48; 4; 0.20]. Mature apothecia sessile to constricted at the base, or somewhat stipitate, (0.15–) 0.31–0.34–0.36 (–0.48) mm high [41; 4; 0.07]. Medulla under the apothecium distinct, (20–) 131–115–162 (–210) μm high [20; 4; 59]; formed of isodiametric to elongated cells, (5.0–) 6.0–9.1–9.5 (–15.0) μm long [44; 4; 2.5] and (3.0–) 5.0–6.1–7.2 (–10.0) μm wide [44; 4; 1.6], or of hyphae (1.5–) 3.0–3.4–3.8 (–5.0) μm wide [36; 4; 0.9]; with polygonal brownish extracellular crystals, (3.0–) 8.4 (–25.0) μm long [17; 1; 5.0] and (3.0–) 6.4 (–12.5) μm wide [17; 1; 3.0]. Disc flat to weakly convex, in mature ascomata raised and with uneven surface, not pruinose. Thalline exciple visible in young apothecia, orange, later inconspicuous but persistent on the lower side of apothecial margin, (23–) 39–84–135 (–222) μm wide in the middle part [38; 7; 44] (measured perpendicular to the outer surface of the exciple, approximately at the midpoint of apothecial height). Cortex of thalline exciple restricted to the lower part, formed of thick-walled intricate paraplectenchyma, of angular cells with lumina (4.0–) 7.2–8.9–11.0 (–15.0) μm long [49; 4; 2.7], and (2.5–) 5.3–6.3–8.5 (–10.0) μm wide [49; 4; 2.3], and with cell walls (1.0–) 1.7–2.1–2.2 (–2.7) μm thick [32; 3; 0.4]. True exciple prominent, persistent, yellow to yellow-orange, always paler than the disk, colourless in inner parts, sometimes weakly cracked in mature apothecia, (15–) 24–29–34 (–50) μm wide [31; 4; 9.8]; formed of thin-walled cells in the uppermost part, (3.0–) 4.4–5.5–6.2 (–10.0) μm long [38; 4; 1.6] and (2.0–) 3.5–4.0–5.0 (–6.0) μm wide [38; 4; 1.0] and of elongated thin-walled cells in the lower part, (4.0–) 6.5–7.0–8.5 (–12.0) μm long [28; 4; 1.7] and (2.0–) 2.5–2.9–3.1 (–5.0) μm wide [28; 4; 0.5]. Hypothecium flat, colourless or sometimes weakly greyish at the base, (13–) 28–30–28 (–70) μm thick [40; 4; 10.6], formed of paraplectenchymatous tissue with thin-walled cells (4.0–) 6.1–6.7–7.0 (–13.0) μm long [48; 4; 1.6], and (2.5–) 4.1–4.8–6.1 (–7.5) μm wide [48; 4; 1.2]. Hymenium colourless, (55–) 66–72–77 (–95) μm high [35; 4; 10.5], with some extracellular oil drops. Paraphyses \pm branched, of thin-walled cells, (1.5–) 1.8–2.8–3.7 (–5.0) μm wide [60; 4; 0.9], but cell walls sometimes glutinized; apical cells swollen (4.0–) 5.8–6.4–7.0 (–9.0) μm wide [61; 4; 1.1]; the number of widening cells below the paraphyses

tips 0–3; the tips always covered by external anthraquinone pigments. Asci clavate, 8-spored, of *Teloschistes* type, (42–) 50–54–56 (–68) μm tall [48; 4; 5], and (10.0–) 11.8–14.0–15.6 (–20.0) μm wide [48; 4; 2.2]. Ascospores polarilocular, (10.0–) 11.7–12.0–12.5 (–14.0) \times (4.0–) 5.0–5.7–6.3 (–8.0) μm [65; 4; 1.1 and 0.9]; length/width ratio (1.37–) 1.99–2.22–2.38 (–3.00) [65; 4; 0.49]; ascospore wall about 0.5–1 μm wide; septa (2.0–) 2.6–3.20–3.13 (–5.0) μm thick [65; 4; 0.82]; ratio of septum width/ascospore length (0.14–) 0.25–0.26–0.30 (–0.45) [65; 4; 0.06]. Ascospores generally ellipsoid, but rhomboid ascospores rarely observed. Pycnidia not seen. Extracellular crystals from all thalline and apothecial parts without reaction with sulphuric acid; (pol+).

***Calogaya xanthoriella* H. Shahidin, species nova**

Mycobank: MB820491

Fig. 5g

Type: CHINA. Xinjiang: Tuo-li, alt. 1450 m, 45°49.003'N, 45.8167166 N, 83.58125E, on twigs of *Berberis heteropoda*, 7 Aug 2008, H. Shahidin 20081344 (**holotype** XJU-NALH).

Type sequences: KY749096 (ITS), KY748768 (beta-tubulin), KY748866 (MS204)

Etymology: Epithet refers to thallus shape that resembles a minute species of *Xanthoria*.

Short diagnosis: Thallus of short-lobed rosettes, but sometimes reduced to squamules around apothecia. Lobes and squamules flat, yellow to greenish yellow. Apothecia small (0.4–0.7 mm diam.), zeorine, distinctly stalked. Disc concave to flat; thalline exciple yellow to orange. Asci with 8 ascospores. Ascospores narrowly to broadly ellipsoid, 9–14 \times 4–7 μm , length/width ratio 1.5–3; ascospore septum 3–5 μm wide, septum width/spore length ratio 0.25–0.42.

Ecology and distribution: Known from montane desert steppes in central Tianshan Mts in China and in mountains of continental Turkey at altitudes 900–2050 m. On bark of shrubs or trees (e.g. *Berberis*, *Lonicera* and *Malus sieversii*) or on weathered wood.

Phylogeny: *Calogaya xanthoriella* forms a supported clade in the single-locus trees (Figs. 1 and 2) and in the concatenated tree (Fig. 3). In the concatenated tree, it is closely related to a lineage consisting of two saxicolous specimens (part of the *C. saxicola* complex) from NW China and southern Siberia. Their sister relation is supported (PP = 0.99). The relationship of their common clade to other *Calogaya* taxa is not resolved. BP&P supported it as a distinct species (Fig. 4).

Detailed description: Thallus crustose, corticolous, squamulose to minutely lobate. Lobes flat, light golden yellow to greenish yellow, very short, (0.05–) 0.1–0.14–0.17 (–0.28) mm long [20; 2; 0.06] and (0.06–) 0.1–0.12–0.14 (–0.29) mm wide [20; 2; 57.4]. Thallus (120–) 140–180–185 (217) μm thick [16; 3; 32.3]. Alveolate cortex (10–) 18.4–20.9–23.4 (–46) μm thick [23; 2; 8.1]; cortex cells \pm round, (4.3–) 7.1–7.4–7.9 (–12.6) \times (3.3–) 5.1–5.6–6.4 (–

11.7) μm [16; 2; 2.3 and 2], cell walls (0.3–) 0.7–0.83–1.0 (–2.4) μm wide [16; 2; 0.48].

Apothecia lecanorine to zeorine, (0.2–) 0.4–0.4–0.6 (–0.7) mm diam. [22; 3; 0.15], apothecial stalks connected at base, of Xanthoriella type (sensu Steiner and Poelt 1982). Disc concave to flat, orange to dark orange, disk surface with yellow pruina, \pm smooth. Thalline exciple paler than disk, bright orange to greenish yellow, mostly hidden below apothecial margin; (41–) 56–59–60 (–98) μm thick in the upper part and (76–) 133–148–153 (–259) μm thick in the lower part [13; 2; 17 and 43]. Cortex of thalline exciple (17–) 29.6–35.6–38.3 (–59) μm in thick [13; 2; 11.1], of oval to polygonal cells, (5.3–) 9.3–10.2–11.7 (–16.4) \times (3.2–) 6.9–7.7–9.1 (–12.6) μm [18; 2; 3. 3&2.7], cell walls 1–2.5 μm thick. True exciple (Parathecium) same colour as disc or paler, 18–58 μm wide, outer part of radiating, oval cells, (6.1–) 6.8–6.8–6.9 (–7.9) \times (5.5–) 5.7–5.7–5.9 (–6.0) μm [7; 2; 0.65 and 0.2]. Inner part (between thalline exciple and hypothecium) (8–) 9.0–12.1–13.1 (24) μm thick [8; 2; 5], of narrow, long and glutinized hyphae. Hymenium colourless, (50–) 58.3–63.2–68.7 (–73.2) μm thick [18; 3; 6.4]. Hypothecium (12–) 17.3–25.3–29.9 (–49) μm thick [21; 3; 9.7], of thin-walled, variously shaped cells, (3.2–) 4.8–5–5.2 (–7.7) \times (2.3–) 3.1–3.3–3.5 (–4.2) μm [5; 1; 1.6 and 0.62]. Paraphyses (1.6–) 2.2–2.3–2.4 (–3.0) μm wide [16; 2; 0.14], usually simple, rarely forked, 1–3 uppermost cells swollen, with oil droplets; tip cells (4–) 5.7–6.3–7.1 (–8.2) μm wide [11; 3; 1.2]. Asci clavate, (37–) 44.9–46.9–47.9 (–58) \times (9–) 10.7–11.3–13.7 (–14) μm [23; 3; 4.8 and 23; 3; 1.6], with 6–8 spores. Ascospores ellipsoid, (8–) 10.6–11.2–12.9 (–16) \times (4–) 5.0–5.2–6.2 (–7) μm [52; 3; 1.57 and 0.76], length/width ratio (1.5–) 2.1–2.2–2.3 (–3.2) [52; 3; 0.31]. Ascospore septum (2.0–) 3.6–3.8–4.0 (–5.0) μm wide [52; 3; 0.65], septum width/spore length ratio (0.2–) 0.31–0.34–0.36 (–0.4) [42; 3; 0.49]. Pycnidia not observed.

***Calogaya xinjiangis* H. Shahidin, species nova**

Mycobank: MB820492

Fig. 5h

Type: CHINA. Xinjiang: Tianshan Great canyon, alt. 3032 m, 43.288633 N, 87.420983, on stem and twigs of *Juniperus pseudosabina*, 11 July 2014, H. Shahidin 144933 (**holotype** XJU-NALH).

Type sequences: KY749024 (ITS), KY748830 (beta-tubulin), KY748946 (MS204)

Etymology: “xinjiangis” is the genitive singular case of the noun Xinjiang, thus meaning “of Xinjiang” (*C. xinjiangis* is only known from Xinjiang).

Short diagnosis: Thallus inapparent or yellow, bullate areolate to subsquamulose, usually surrounding young apothecia. Apothecia numerous, zeorine, 0.5–1.0 mm diam., usually grouped, stalked. Disc bright orange, thalline exciple yellow. Asci with 8 ascospores. Ascospores 8–14 \times 5–9 μm , length/

width ratio 1.8–2.3. Ascospore septum 2.5–4 μm wide, septum width/spore length ratio 0.19–0.34.

Ecology and distribution: Known from two localities in Tianshan Mts (NW China, Xinjiang) in montane/subalpine steppes, at altitudes 2500–3000 m). Growing on bark of *Juniperus centralasiatica* and *J. pseudosabina*.

Phylogeny: *Calogaya xinjiangis* forms a supported clade in the single-locus trees (Figs. 1 and 2) and in the concatenated tree (Fig. 3). Its relationships to other *Calogaya* taxa are unresolved. BP&P supported it as a distinct species (Fig. 4).

Detailed description: Thallus crustose, corticolous, inconspicuous or forming bullate areoles or small squamules surrounding young apothecia, orange to greenish yellow. Areoles/squamules (0.09–) 0.11–0.16–0.2 (–0.26) mm diam. [19; 3; 45.7]; thallus (35–) 79.4–88–98.4 (–127) μm thick [20; 2; 23.2]. Cortex uneven, (8.3–) 18–20–22 (–31) μm thick [17; 2; 6.5], alveolate, of cells (5.7–) 7.9–8.9–9.9 (–10.4) \times (3.4–) 5.6–6.7–7.9 (–9) μm [14; 2; 1.4 & 1.8]; cell walls (0.56–) 0.92–0.98–1.1 (–1.3) μm wide [14; 2; 0.21]. Algal layer discontinuous, (41–) 51.2–57.3–69.5 (–76) μm thick [9; 2; 11.5], algal cells (10–) 12.6–14.5–15.5 (–22) \times (8–) 9.7–12.4–13.5 (–18.3) μm [16; 2; 2.8 and 2.5].

Apothecia abundant, (0.23–) 0.46–0.52–0.77 (–1.25) mm diam. [28; 3; 0.2], usually grouped, along fissures in substrate, stipitate, bright orange, zeorine. Disk plane to convex, dark orange to ferruginous orange. Thalline exciple prominent and bright orange in young apothecia, but reduced and hidden below margin in older apothecia; (37–) 64–73–81 (–105) μm thick in the upper part and (102–) 126–144–160 (–198) μm thick in the lower part [15; 2; 18 and 27]. Cortex of thalline exciple (12.3–) 23.4–29.4–49.1 (–59.6) μm [25; 3; 12.6], cortex cells with tiny oil droplets, of cells (5–) 9.3–11.1–13.3 (–18.8) \times (2.7–) 6.2–7.5–9.3 (–13.7) μm [30; 3; 3.5 and 3], cell walls (0.49–) 0.95–1.25–1.64 (–2.7) μm wide [30; 3; 0.5]. True exciple (parathecium) well developed, coloured as disk in mature apothecia, but yellow in young apothecia, (35.4–) 40.8–52.3–59.2 (–76.9) μm wide [14; 3; 11.1], consisting of radiating oval cells (4.3–) 6.9–7.4–8.3 (–13.1) \times (4–) 4.9–5.5–6.7 (–7.8) μm [18; 3; 2.3 and 1], cell walls (0.43–) 0.98–1–1.03 (–1.5) μm wide [14; 2; 0.3], lumina with oil droplets. Lower part of true exciple (forming a belt of cells between the thalline exciple and hypothecium) (7–) 9.9–15.3–18.3 (–23) μm thick [18; 3; 3.9], of long and narrow hyphae. Hymenium colourless, (45–) 51.3–63.1–80.2 (–91) μm thick [17; 3; 14.8]. Hypothecium interspersed, colourless, (14–) 32–33–37.8 (–60) μm in high [20; 3; 10.5], of cells (3.4–) 6.1–6.6–7.6 (–13.3) \times (2.2–) 3–4.2–5 (9.2) μm [22; 3; 3 and 1.6], with oil droplets. Medulla below apothecia strongly developed. Paraphyses (1.6–) 2–2.2–2.3 (–2.9) μm wide [36; 3; 0.29], usually simple, rarely forked near tips, tip cells swollen, (4.3–) 5.6–6.3–7.1 (–8.6) μm wide [23; 3; 1.2], with oil drops. Asci 8-spored, (42–) 49.4–52.7–57 (–64) \times (9–) 14.2–14.8–15.6 (–19.5) μm [26; 3; 6.1 and 2.4], length/

width ratio (2.26–) 3.2–3.7–4.2 (–6.78) [26; 3; 0.94]. Ascospores (7.2–) 11.3–11.5–11.7 (–14.6) × (4.7–) 6.1–6.7–7.2 (–9.5) μm [50; 3; 1.9 and 1], length/width ratio (1.13–) 1.64–1.73–1.91 (–2.4) [50; 3; 0.32], spore wall (0.4–) 0.68–0.7–0.74 (–1) μm wide [29; 3; 0.18]. Ascospore septum (2.2–) 2.83–2.9–3 (–3.9) μm wide [50; 3; 0.47], septum width/spore length ratio (0.18–) 0.25–0.26–0.26 (–0.38) [50; 3; 0.045]. Pycnidia not observed.

New combinations

Calogaya polycarpoides* subsp. *persica (J. Steiner) M. Haji Moniri & Vondrák, **combinatio nova**

Mycobank: MB820493

≡ *Xanthoria polycarpoides* var. *persica* J. Steiner, *Annales Mycologici* 8:241. 1910.

Type: IRAN. Arak Province, Gulpeighan [Golpayegan], 33.53°N, 50.30°E, on *Salix* bark, 1905/1906, *Th. Strauss* (lectotype W, not seen).

Commentary: Steiner and Poelt (1982) considered *Caloplaca* (= *Calogaya*) *persica* and *C. polycarpoides* as two distinct species that are only distinguished by the number of ascospores in asci. Both taxa are epiphytic, known mainly from dry regions of western Asia. Our single-gene and concatenated phylogenies (Figs 2 and 3) did not recognise the two taxa that commonly grow in the same locality (even on the same tree). BP&P found no significant solution for its status but found higher probability for treating the two taxa as a separate species than for merging them into a single species (Fig. 4). Identical ecology, almost identical morphology and the observed genetic similarity are reasons for their recognition as infraspecific taxa. However, the increased number of ascospores in asci of subsp. *persica* is a unique character in *Calogaya* and may have evolutionary potential. Kondratyuk et al. (2013) reported 8–16 ascospores in asci also in *Caloplaca* (= *Calogaya*) *zoroasteriorum*, but his counts came probably from apothecia of *C. persica* as both species are commonly intermixed. (*C. zoroasteriorum* is rarely fertile and we observed only 8-spored asci in this species.)

Calogaya zoroasteriorum (S.Y. Kondr., Kärnefelt, A. Thell, Elix, J. Kim, A.S. Kondratiuk & J.-S. Hur) M. Haji Moniri & Vondrák, **combinatio nova**

Mycobank: MB820494

≡ *Lazarenkoella zoroasteriorum* S.Y. Kondr., Kärnefelt, A. Thell, Elix, J. Kim, A.S. Kondr. & Hur, in Kondratyuk, Kärnefelt, Thell, Elix, Kim, Kondratiuk & Hur, *Acta botanica hungarica* 57, p. 340. 2015.

≡ *Caloplaca zoroasteriorum* S. Y. Kondr. & M. Haji Moniri, *Acta Botanica Hungarica* 55(1–2):56–59 2013. (Illegitimate name).

Type: IRAN. Razavi Khorasan province: West of Torbat-e Heidarieh, Baig, Rudmaajan, close to waterfall, on bark of

Prunus sp. Lat.; 35.455328°N, 58.839282°E; Alt.; 1118 m, 15 Sept 2012, *F. Hooshmand* and *M. Haji Moniri* 2481 (holotype TARI).

Commentary: Based on our DNA sequence data from four specimens (including one paratype), this distinct soresiate species (Kondratyuk et al. 2013) is placed in *Calogaya*. In the concatenated tree, it forms two close lineages but without supported sister relationship (Fig. 3). In single-locus ITS and beta-tubulin trees, sequences of *C. zoroasteriorum* group together, but with no support (Figs 1 and 2). BP&P revealed no significant solution for the status of the two lineages of *C. zoroasteriorum*, but it found higher probability for recognising them as separate species than for merging them into a single species (Fig. 4). Because of their similar morphology and ecology, we decided to merge specimens of both lineages under the name *C. zoroasteriorum*, although two taxa may be included.

Kondratyuk et al. (2015a) accommodated the species in the new monotypic genus *Lazarenkoella* belonging to a different subfamily *Brownlielloideae*, but the genus and the whole subfamily was described on the basis of a hybrid dataset of DNA sequences: their concatenated dataset contained ITS and nrLSU loci from the lichen mycobiont, but mtSSU from a fungal contaminant. Furthermore, *Lazarenkoella* was established on the basis of lichens that are not *C. zoroasteriorum*. It was based on the DNA data of specimens SK A45, SK A51 and SK A55. ITS sequences from the first two belong to *Calogaya*, but to another taxon (*C. polycarpoides* which is often present together with specimens of *C. zoroasteriorum*). ITS sequence from SK A55 belongs to *Gyalolechia* (possibly a mistake or contamination in laboratory).

Acknowledgments Linda in Arcadia kindly revised the manuscript. We acknowledge generous support from the National natural science foundation of China (NFSC, projects no. 31093440 and no. 31260008) and a long-term research development grant RVO 67985939.

References

- Aras S, Cansaran D (2006) Isolation of DNA for sequence analysis from herbarium material of some lichen specimens. *Turk J Bot* 30:449–453
- Arcadia L (2009) Large genera, small genera and lichen taxonomy. *Br Lichen Soc Bull* 104:13–19
- Arup U, Søchting U, Frödén P (2013) A new taxonomy of the family Teloschistaceae. *Nord J Bot* 31:16–83
- Bässler C, Cadotte MW, Beudert B, Heibl C, Blaschke M, Bradtka JH, Langbehn T, Werth S, Müller J (2015) Contrasting patterns of lichen functional diversity and species richness across an elevation gradient. *Ecography* 38:1–10
- Crespo F, Kauff PK, Divakar R, del Prado S, Pérez-Ortega S, de Paz GA, Ferencova Z, Blanco O, Roca-Valiente B, Núñez-Zapata J, Cubas P, Argüello A, Elix JA, Esslinger TL, Hawksworth DL, Millanes AM, Molina MC, Wedin M, Ahti T, Aptroot A, Barreno E, Bungartz F,

- Calvelo S, Candan M, Cole MJ, Ertz D, Goffinet B, Lindblom L, Lücking R, Lutzoni F, Mattsson JE, Messuti MI, Miadlikowska J, Piercey-Normore MD, Rico VJ, Sipman H, Schmitt I, Spribille T, Thell A, Thor G, Upreti DK, Lumbsch HT (2010) Phylogenetic generic classification of parmelioid lichens (Parmeliaceae, Ascomycota) based on molecular, morphological and chemical evidence. *Taxon* 59:1735–1753
- Drummond AJ, Rambaut A (2007) BEAST: Bayesian evolutionary analysis by sampling trees. *BMC Evol Biol* 7:214
- Ekman S (1996) The corticolous and lignicolous species of *Bacidia* and *Bacidina* in North America. *Opera Bot* 127:1–148
- Frolov I, Vondrák J, Fernández-Mendoza F, Wilk K, Khodosovtsev A, Halıcı MG (2016) Three new, seemingly-cryptic species in the lichen genus *Caloplaca* (Teloschistaceae) distinguished in two-phase phenotype evaluation. *Ann Bot Fenn* 53:243–262
- Gardes M, Bruns TD (1993) ITS primers with enhanced specificity for basidiomycetes—application for the identification of mycorrhizae and rusts. *Mol Ecol* 2:113–118
- Gaya E (2009) Taxonomical revision of the *Caloplaca saxicola* group (Teloschistaceae, lichen-forming Ascomycota). *Bibl Lichenol* 101:1–191
- Gaya E, Redelings BD, Navarro-Rosinés P, Llimona X, De Cáceres M, Lutzoni F (2011) Align or not to align? Resolving species complexes within the *Caloplaca saxicola* group as a case study. *Mycologia* 103:361–378
- Gaya E, Fernández-Brime S, Vargas R, Lachlan RF, Gueidan C, Ramírez-Mejía M, Lutzoni F (2015) The adaptive radiation of lichen-forming Teloschistaceae is associated with sunscreens pigments and a bark-to-rock substrate shift. *PNAS* 112:11600–11605
- Hall TA (1999) BioEdit: a user-friendly biological sequence alignment editor and analysis program for Windows 95/98/NT. *Nucleic Acids Symp Ser* 41:95–98
- Huelsensbeck JP, Ronquist F (2001) MrBayes: Bayesian inference of phylogeny. *Bioinformatics* 17:754–755
- Johansson V, Ranius T, Snäll T (2012) Epiphyte metapopulation dynamics are explained by species traits, connectivity, and patch dynamics. *Ecology* 93:235–241
- Johansson V, Ranius T, Snäll T (2013) Epiphyte metapopulation persistence after drastic habitat decline and low tree regeneration: time-lags and effects of conservation actions. *J Appl Ecol* 50:414–422
- Katoh K, Standley DM (2013) MAFFT multiple sequence alignment software version 7: improvements in performance and usability. *Mol Biol Evol* 30:772–780
- Katoh K, Kuma K, Toh H, Miyata T (2005) MAFFT version 5: improvement in accuracy of multiple sequence alignment. *Nucleic Acids Res* 33:511–518
- Kondratyuk SY, Lökös L, Zarei-Darki B, Haji Moniri M, Tchabanenko S, Galanina I, Yakovchenko L, Hooshmand F, Ezhkin A, Hur J-S (2013) Five new *Caloplaca* species (Teloschistaceae, Ascomycota) from Asia. *Acta Bot Hungar* 55:41–60
- Kondratyuk SY, Kärnefelt I, Thell A, Elix JA, Kim J, Jeong M-H, Yu N-N, Kondratiuk A, Hur J-S (2014a) A revised taxonomy for the subfamily Xanthorioideae (Teloschistaceae, Ascomycota) based on molecular phylogeny. *Acta Bot Hungar* 56:141–178
- Kondratyuk SY, Jeong M-H, Yu N-N, Kärnefelt I, Thell A, Elix JA, Kim J, Kondratiuk AS, Hur J-S (2014b) A revised taxonomy for the subfamily Caloplacoideae (Teloschistaceae, Ascomycota) based on molecular phylogeny. *Acta Bot Hungar* 56:93–123
- Kondratyuk SY, Kärnefelt I, Thell A, Elix JA, Kim J, Kondratiuk AS, Hur J-S (2015a) Brownlielloideae, a new subfamily in the Teloschistaceae (Lecanoromycetes, Ascomycotina). *Acta Bot Hungar* 57:321–343
- Kondratyuk SY, Lökös L, Kim JA, Kondratiuk AS, Jeong MH, Jang SH, Oh S-O, Hur J-S (2015b) Three new monotypic genera of the Caloplacoid lichens (Teloschistaceae, lichen-forming ascomycetes). *Mycobiology* 43:195–202
- Lücking R (2008) Foliicolous lichenized Fungi. *Flora Neotropica Monograph* 103:1–866
- Magnusson AH (1940) Lichens from Central Asia. Part I. In: Hedin S (ed) Reports Scientific Exped. North-west. provinces of China (the Sino-Swedish expedition). 13, XI. Botany, 1. Aktiebolaget Thule, Stockholm
- Magnusson AH (1944) Lichens from Central Asia. Part II. In: Hedin S (ed) Reports Scientific Exped. Northwest. provinces of China (the Sino-Swedish Expedition). 22, XI, Botany, 2. Aktiebolaget Thule, Stockholm
- Myllys L, Lohtander K, Tehler A (2001) β -tubulin, ITS and group I intron sequences challenge the species pair concept in *Physcia aipolia* and *P. caesia*. *Mycologia* 93:335–343
- Nelson PR, McCune B, Roland C, Stehn S (2015) Non-parametric methods reveal non-linear functional trait variation of lichens along environmental and fire age gradients. *J Veg Sci* 26:848–865
- Posada D (2008) jModelTest: phylogenetic model averaging. *Mol Biol Evol* 25:1253–1256
- Rambaut A, Drummond AJ (2009) TreeAnnotator. Available online at <http://beast.bio.ed.ac.uk/TreeAnnotator>
- Rambaut A, Suchard MA, Xie D, Drummond AJ (2014) Tracer v1.6. Available online at <http://beast.bio.ed.ac.uk/Tracer>
- Rannala B, Yang Z (2003) Bayes estimation of species divergence times and ancestral population sizes using DNA sequences from multiple loci. *Genetics* 164:1645–1656
- Ronquist F, Huelsenbeck JP (2003) MrBayes 3: Bayesian phylogenetic inference under mixed models. *Bioinformatics* 19:1572–1574
- Shahidin H, Abbas A, Wei J (2010) *Caloplaca tianshanensis* (lichen-forming Ascomycota), a new species of subgenus *Pyrenodesmia* from China. *Mycotaxon* 114:1–6
- Simmons MP, Ochoterena H (2000) Gaps as characters in sequence-based phylogenetic analyses. *Syst Biol* 49:369–381
- Smith CW, Aptroot A, Coppins BJ, Fletcher A, Gilbert OL, James PW, Wolsley PA, eds (2009) *The Lichens of Great Britain and Ireland*. British Lichen Society, London
- Søchting U, Figueras G (2007) *Caloplaca lenae* species nova, and other *Caloplaca* species with caloploicin and vicanicin. *Lichenologist* 39:7–14
- Søchting U, Garrido-Benavent I, Seppelt R, Castello M, Pérez-Ortega S, de los Ríos Murillo A, Frödén P, Arup U (2014a) *Charcotiana* and *Amundsenia*, two new genera in Teloschistaceae (lichenized Ascomycota, subfamily Xanthorioideae) hosting two new species from continental Antarctica, and *Austroplaca frigida*, a new name for a continental Antarctic species. *Lichenologist* 46:763–782
- Søchting U, Sogaard MZ, Elix JA, Arup U, Elvebakk A, Sancho LG (2014b) *Catenarina* (Teloschistaceae, Ascomycota), a new southern hemisphere genus with 7-chlorocatenarin. *Lichenologist* 46:175–187
- Sokal RR, Sneath PHA (1963) *Principles of numerical taxonomy*. W.H. Freeman, San Francisco
- Stamatakis A, Ludwig T, Meier H (2005) RAXML-III: a fast program for maximum likelihood-based inference of large phylogenetic trees. *Bioinformatics* 21:456–463
- Steiner M, Poelt J (1982) *Caloplaca* sect. *Xanthoriella*, sect. nov.: Untersuchungen über die “*Xanthoria lobulata*-Gruppe” (Lichenes, Teloschistaceae). *Plant Syst Evol* 140:151–177
- Sukumar J, Knowles LL (2017) Multispecies coalescent delimits structure, not species. *PNAS* 114:1607–1612
- Tehler A, Ertz D, Irestedt M (2013) The genus *Dirina* (Roccellaceae, Arthoniales) revisited. *Lichenologist* 45:427–476
- Veselská T, Svoboda J, Růžicková Z, Kolařík M (2014) Application of flow cytometry for genome size determination in Geosmithia fungi: a comparison of methods. *Cytometry A* 85:854–861
- Vondrák J, Khodosovtsev A, Šoun J, Vondráková O (2012) Two new European species from the heterogeneous *Caloplaca holocarpa* group (Teloschistaceae). *Lichenologist* 44:73–89

- Vondrák J, Frolov I, Arup U, Khodosovtsev A (2013a) Methods for phenotypic evaluation of crustose lichens with emphasis on *Teloschistaceae*. *Chernomorsky Botanicheskii Zhurnal* 9:382–405
- Vondrák J, Frolov I, Říha P, Hrouzek P, Palice Z, Nadyeina O, Halıcı G, Khodosovtsev A, Roux C (2013b) New crustose *Teloschistaceae* in Central Europe. *Lichenologist* 45:701–722
- Vondrák J, Frolov I, Davydov EA, Urbanavichene I, Chesnokov S, Zhdanov I, Muchnik E, Konoreva L, Himelbrant D, Tchabanenko S (2016) The extensive geographical range of several species of *Teloschistaceae*: evidence from Russia. *Lichenologist* 48:171–189
- Yang Z (2015) The BPP program for species tree estimation and species delimitation. *Curr Zool* 61:854–865
- Yang Z, Rannala B (2010) Bayesian species delimitation using multilocus sequence data. *PNAS* 107:9264–9269
- Yang Z, Rannala B (2014) Unguided Species Delimitation Using DNA Sequence Data from Multiple Loci. *Mol Biol Evol* 31:3125–3135